Table 4. Summary of Spi^- mutant frequencies in the lung of *gpt* delta rats treated with Ni_3S_2 by intratracheal administration and liver treated with ENU (positive control)

Treatment	Smpling time	Animal No.	Organ	Number of packagings	Total Population	Number of mutants	Mutant frequency ($\times 10^{-6}$)	
								Mean ± SD
0 mg/animal × 4	28 days	1001	lung	6	865,500	5	5.78	
		1002	lung	6	1,665,000	4	2.40	
		1003	lung	6	1,224,000	9	7.35	
		1004	lung	6	951,000	4	4.21	
		1005	lung	6	1,339,500	17	12.69	6.49 ± 3.93
0.5 mg/animal × 4	28 days	1101	lung	4	631,500	3	4.75	
		1102	lung	6	1,412,500	7	4.96	
		1103	lung	6	656,000	3	4.57	
		1104	lung	5	622,500	2	3.21	
		1105	lung	5	1,426,500	8	5.61	4.62 ± 0.88
1 mg/animal × 4	28 days	1201	lung	6	1,188,000	8	6.73	
		1202	lung	6	1,371,000	8	5.84	
		1203	lung	7	7 23,000	5	6.92	
		1204	lung	7	456,000	6	13.16	
		1205	lung	6	1,570,500	14	8.91	8.31 ± 2.93
0 mg/animal × 4	90 days	1011	lung	3	697,500	3	4.30	
		1012	lung	4	550,500	4	7.27	
		1013	lung	4	1,380,000	2	1.45	
		1014	lung	3	1,314,000	10	7.61	
		1015	lung	3	1,620,000	8	4.94	5.11 ± 2.50
0.5 mg/animal × 4	90 days	1111	lung	3	1,225,500	9	7.34	
		1112	lung	4	1,212,000	9	7.43	
		1113	lung	3	1,692,000	9	5.32	
		1114	lung	4	708,000	4	5.65	
		1115	lung	3	1,380,000	6	4.35	6.02 ± 1.34
1 mg/animal × 4	90 days	1211	lung	6	1,110,000	3	2.70	
		1212	lung	3	1,063,500	4	3.76	
		1213	lung	3	1,012,500	5	4.94	
		1214	lung	4	946,500	6	6.34	
		1215	lung	5	2,233,500	7	3.13	4.18 ± 1.47
ENU	31 days	51	liver	1	547,500	10	18.26	
50 mg/kg × 5		52	liver	1	478,500	4	8.36	
		53	liver	1	357,000	3	8.40	
		54	liver	1	219,000	4	18.26	
		55	liver	1	460,500	14	30.40	16.74 ± 9.10†

†The Spi^- MF in the livers of *gpt* delta rats treated with ENU was markedly increased compared to the spontaneous Spi^- MF in F344 *gpt* delta rat livers of 2.8×10^{-6} previously reported (7).

Table 5. Histopathological results in the lung of Ni_3S_2-treated male F344 *gpt* delta rats

Group	Sampling time	No. of animals	Infiltration of inflammatory cells (including eosinophils, perivascular)	Fibrosis (focal)	Infiltration of alveolar macrophages
Ni_3S_2 0 mg × 4	28 days	5	5 (2+)		
Ni_3S_2 0.5 mg × 4	28 days	5	5 (2+)	2 (1+)	
Ni_3S_2 1 mg × 4	28 days	5	5 (2+)	2 (1+)	3* (1(1+), 2(2+))
Ni_3S_2 0 mg × 4	90 days	5	4 (1+)		
Ni_3S_2 0.5 mg × 4	90 days	5	3 (1+)	1 (1+)	
Ni_3S_2 1 mg × 4	90 days	5	1 (1+)		

The number of the animals bearing the lesion in each exposed or control group were shown in the column. The parenthesized values indicate the number of the animals bearing the lesion with each of 4 different grades of severity, i.e., 1+: slight, 2+: moderate, 3+: marked, 4+: severe. Significant difference indicated by $^*p \leqq 0.05$ by Fisher exact test compared to each control.

Discussion

The lung inflammation induced with the higher dose of Ni_3S_2 was characterized by the infiltration of alveolar macrophages and, furthermore, the fibrosis was observed in the both of Ni_3S_2-treated groups. These lung lesions indicated an inflammation and recovery from the inflammation. The histopathological results at 90-days suggested the recovery of inflammatory lesions. Similar results were obtained in lung toxicity study after 13-week inhalation exposure to Ni_3S_2 in F344 rats and mice (47). These results suggested that the treatment of conditions of the present study ensured that the rats were sufficiently challenged by Ni_3S_2 particles. And the period of sampling time was long enough to detect mutations because regeneration and/or recovery were observed in the lung tissues of the Ni_3S_2-treated groups at 28 or 90 days after the first treatment. In addition, a threshold of insoluble particles in lung clearances of F344 rats was estimated at 1–2 mg (45). The impaired lung clearance with overload of particles might induce tumor and fibrosis (48).

The *gpt* MFs in the lung were independently measured in four independent laboratories using a common standard method. The overall packaging efficiencies in each laboratory tended to be low, especially in one laboratory. One of the reasons was thought to poor DNA quality extracted. In addition, copy number of the transgene in transgenic animals may affect efficiency of recovery of the transgene. It is reasonable that *gpt* delta rat assays need more packaging than mouse assays, because copy number of the transgene par haploid is $5 \sim 10$ in rat and about 80 in mouse (4,5). Another reason might be lower activity of packaging extract used.

The *gpt* MFs obtained by the four laboratories were similar, without any statistical differences between any of the laboratories. Administration of 0.5 or 1 mg Ni_3S_2/rat once a week for four weeks did not affect *gpt* MF in the lungs of F344 *gpt* delta rats: the *gpt* MFs were all similar to the previously reported spontaneous *gpt* MF in the lungs of *gpt* delta mice (3.4×10^{-6}) (7). Further, no increase in the Spi MF was observed in the treated groups.

Ni_3S_2 is able to interact with molecular oxygen and generate reactive oxygen species (ROS) (27), and Kawanishi *et al.* (40) reported that Ni_3S_2 induced pathological inflammation and oxidative DNA damage in the lungs of rats treated with single intratracheal instillation of 0.5 or 1.0 mg/animal. Ni_3S_2 generation of DNA-damaging ROS coupled with induction of inflammation and its inhibition of DNA repair is thought to enhance its genotoxicity and tumorigenicity (27,40). This suggests that F344 *gpt* delta rats exposed by intratracheal instillation to high doses of Ni_3S_2 should acquire multiple mutations in the lung. In our study, however, although F344 *gpt* delta rats were administered Ni_3S_2 at doses high enough to induce inflammatory responses in the lung and the duration of the experiment was set as weekly dosing for four weeks with two sampling periods (28 or 90 days after the first treatment), Ni_3S_2 did not cause an increase in *gpt* or Spi^- MF in the lung. The lack of induction of mutation is in agreement with the resultsof *in vitro* mutagenesis assays (20,27–29,36–38). Moreover, administration of Ni_3S_2 by inhalation to the Muta™ Mouse and the Big Blue® rat did not induce mutations in the *lacZ* or the *lacI* genes (41). Taken together, these data suggest that *in vivo* mutagenicity of Ni_3S_2, such as induction of point mutations or small deletions, could not be observed by transgenic rodent mutation assays under those experimental conditions.

One possible reason why ROS-induced DNA damage does not lead to a detectable increase in mutations is that the damages are eliminated, either by the damage being repaired or by the cells undergoing apoptosis. Various studies have demonstrated that ROS induced by toxic metals are closely related to metal-induced apoptosis and carcinogenesis (49). Inhalation of high concentrations of amosite asbestos and bitumen fume by rats induces oxidative DNA damage (50–52). In the Big Blue® rat, a single intratracheal instillation of amosite asbestos 20–30 μm in length at a dose of 2 mg/animal resulted in a 2-fold increase in DNA mutations 16 weeks after treatment (53). In these animals, however, the amosite fibers were not eliminated from the lung and caused significant tissue damage with infiltration of neutrophils and macrophages. It is well known that long ($>10\,\mu$m) asbestos fibers induce ROS generation by phagocytes (54–56). Therefore, ROS generation stimulated by asbestos was augmented by neutrophils and macrophages, and the production of ROS continued throughout the experiment. In contrast to asbestos fibers, bitumen fumes, which did not cause prolonged inflammation or prolonged infiltration of phagocytes, did not induce an increase in MFs in the lungs of Big Blue® rats despite the formation of DNA adducts (50).

Two other genotoxic mechanisms may contribute to the carcinogenicity of Ni_3S_2 in the rat lung. Recently, it was demonstrated that Ni_3S_2 induced silencing of the *gpt* transgene present in G12 cells, a V79-derived transgenic Chinese hamster cell line containing the *gpt* transgene, without mutation of the transgene (57). The silencing of the *gpt* gene was shown to be due to DNA methylation. If DNA hypermethylation results in aberrant silencing of a tumor suppressor gene, it could participate in carcinogenesis (27,41,57). This type of epigenetic event would not be detected by the *gpt* or Spi^- assays we used to detect Ni_3S_2 induced mutations.

Another genotoxic mechanism is the generation of chromosomal breaks leading to mutations such as DNA strand breaks which lead to chromosomal aberrations. This type of damage will be rarely detected by the *gpt* or

Spi$^-$ assays we used to detect Ni_3S_2 induced mutations. For example, a single administration of Ni_3S_2 by nose only inhalation for 2 h at concentrations of 86 and 130 Ni_3S_2 mg/m^3 to Muta^{TM} mice and Big Blue® rats (estimated doses of 6 and 10 mg/kg) did not cause increased mutations in nasal or lung mucosa despite clear induction of DNA strand breaks (41).

Another possibility is that the *gpt* or Spi$^-$ assays we used to detect Ni_3S_2 induced mutations were not sensitive enough to detect Ni_3S_2 generated mutations in the lung. Mutations are fixed into the genome of a cell primarily through DNA replication. Therefore, the population of stem cells in an organ is important for mutational events to occur, associating the sensitivity of an organ to a mutagen with the organ's population of stem cells and their cell division rate (16,58–60). Consequently, the primary target cells of Ni_3S_2 mutagenicity and carcinogenicity in the lung are epithelial type II cells, the lung stem cells. However, these cells make up only 12% of total alveolar cell population in 5-month-old male rats (61). In the liver, a tissue in which increases in *gpt* and Spi$^-$ MFs were readily detected, over 80% of the mass of the organ is made up of liver stem cell hepatocytes (62). Therefore, the low sensitivity to the Ni_3S_2 mutagenicity in the lung of transgenic rodents might be due to the low population of stem cells. In addition, the lung has a well developed antioxidant system and this would decrease the mutagenicity of ROS generating genotoxic compounds (63). Dimethylarsinic acid (DMA) induces DNA damage in the lung by formation of peroxyl radical species; however, DMA was ineffective in inducing mutations in the lungs of Muta^{TM} Mice (64). The authors speculate that the mutagenicity of DMA in the lung might be too low to be detected in the Muta^{TM} Mouse. Of course, as noted above, the lack of mutagenicity may have been due to removal of cells harboring DNA damage. On the other hand, when kaolin, manufactured insoluble micro/nanoparticles which induce lung carcinogenesis in rodents, were intratracheally instilled into *gpt* delta mice, they caused 2-fold increases in *gpt* and Spi$^-$ MFs in the lung (13). Other studies also reported the increase in *gpt* MFs in the lung of *gpt* delta mice treated with benzo[a]pyrene or 1,6-dinitropyrene by a single intratracheal instillation and diesel exhaust by inhalation for 24 weeks (65–67). Those suggest that the *gpt* and Spi$^-$ assays using *gpt* delta transgenic animals are sensitive enough to detect an increased MF if it exists.

Briefly, possible reasons why we could not detect mutations in the lungs of F344 *gpt* delta rats exposed to the carcinogen Ni_3S_2 are (1) Ni_3S_2 exerts its effects by a non-genotoxic mechanism; (2) the type of mutation induced by Ni_3S_2 could not be detected by the *gpt* or Spi$^-$ assays; (3) the type of mutation induced by Ni_3S_2 could be detected by the *gpt* and Spi$^-$ assays, but these assays are not sensitive enough to detect mutations under the experimental condition we used.

Investigation of genotoxic effects in a target organ after exposure to a compound *in vivo* is critical for understanding the mechanism of carcinogenicity and for risk assessment of carcinogens. Consequently, the transgenic rodent mutation assay has become a critically important method of investigating the effects which carcinogens have on the various organs of the body. Validation of an existing system or development of a new system for determining mutagenicity in the lung is critically important to determine the risk of workplace and environmental pollutants and to properly regulate the generation of hazardous materials.

In conclusion, the results of our study indicate that Ni_3S_2 does not induce the *gpt* or Spi$^-$ mutations in the lung of *gpt* delta rats. Therefore, this assay evaluates Ni_3S_2 as non-mutagenic in the lung of F344 *gpt* delta transgenic rats. The results obtained by four different laboratories were consistent. If the protocol is effective in measuring the mutations which occur in the target organ, it can be used to investigate the mutagenic potential of test compounds by independent laboratories. Further studies, however, are required to validate this transgenic rodent mutation assays for use in evaluating *in vivo* mutagenicity in the target organ.

Acknowledgments: We wish to express our thanks to Dr. David B. Alexander, Graduate School of Medical Sciences, Nagoya City University, for proofreading this manuscript.

References

1 Kohler SW, Provost GS, Kretz PL, Fieck A, Sorge JA, Short JM. The use of transgenic mice for short-term, *in vivo* mutagenicity testing. Genet Anal Tech Appl. 1990; 7: 212–8.

2 Dycaico MJ, Provost GS, Kretz PL, Ransom SL, Moores JC, Short JM. The use of shuttle vectors for mutation analysis in transgenic mice and rats. Mutat Res. 1994; 307: 461–78.

3 Gossen JA, de Leeuw WJ, Tan CH, Zwarthoff EC, Berends F, Lohman PH, Knook DL, Vijg J. Efficient rescue of integrated shuttle vectors from transgenic mice: a model for studying mutations *in vivo*. Proc Natl Acad Sci USA. 1989; 86: 7971–5.

4 Nohmi T, Katoh M, Suzuki H, Matsui M, Yamada M, Watanabe M, Suzuki M, Horiya N, Ueda O, Shibuya T, Ikeda H, Sofuni T. A new transgenic mouse mutagenesis test system using Spi$^-$ and 6-thioguanine selections. Environ Mol Mutagen. 1996; 28: 465–70.

5 Hayashi H, Kondo H, Masumura K, Shindo Y, Nohmi T. Novel transgenic rat for *in vivo* genotoxicity assays using 6-thioguanine and Spi$^-$ selections. Environ Mol Mutagen. 2003; 41: 253–9.

6 Nohmi T, Suzuki T, Masumura K. Recent advances in the

protocols of transgenic mouse mutation assays. Mutat Res. 2000; 455: 191–215.
7 Masumura K. Spontaneous and induced *gpt* and Spi$^-$ mutant frequencies in *gpt* delta transgenic rodents. Genes Environ. 2009; 31: 105–18.
8 Masumura K, Matsui M, Katoh M, Horiya N, Ueda O, Tanabe H, Yamada M, Suzuki H, Sofuni T, Nohmi T. Spectra of *gpt* mutations in ethylnitrosourea-treated and untreated transgenic mice. Environ Mol Mutagen. 1999; 34: 1–8.
9 Okada N, Masumura K, Nohmi T, Yajima N. Efficient detection of deletions induced by a single treatment of mitomycin C in transgenic mouse *gpt* delta using the Spi(−) selection. Environ Mol Mutagen. 1999; 34: 106–11.
10 Masumura K, Matsui K, Yamada M, Horiguchi M, Ishida K, Watanabe M, Ueda O, Suzuki H, Kanke Y, Tindall KR, Wakabayashi K, Sofuni T, Nohmi T. Mutagenicity of 2-amino-1-methyl-6-phenylimidazo[4,5-*b*]pyridine (PhIP) in new *gpt* delta transgenic mouse. Cancer Lett. 1999; 143: 241–4.
11 Nohmi T, Suzuki M, Masumura K, Yamada M, Matsui K, Ueda O, Suzuki H, Katoh M, Ikeda H, Sofuni T. Spi(−) selection: An efficient method to detect gamma-ray-induced deletions in transgenic mice. Environ Mol Mutagen. 1999; 34: 9–15.
12 Okudaira N, Uehara Y, Fjikawa K, Kagawa N, Ootsuyama A, Norimura T, Saeki K, Nohmi T, Masumura K, Matsumoto T, Oghiso Y, Tanaka K, Ichinohe K, Nakamura S, Tanaka S, Ono T. Radiation dose-rate effect on mutation induction in spleen and liver of *gpt* delta mice. Radiat Res. 2010; 173: 138–47.
13 Totsuka Y, Higuchi T, Imai T, Nishikawa A, Nohmi T, Kato T, Masuda S, Kinae N, Hiyoshi K, Ogo S, Kawanishi M, Yagi T, Ichinose T, Fukumori N, Watanabe M, Sugimura T. Genotoxicity of nano/microparticles in *in vivo* micronuclei, *in vivo* comet and mutation assay system. Part Fibre Toxicol. 2009; 3: 6–23.
14 Heddle JA, Dean S, Nohmi T, Boerrigter M, Casciano D, Douglas GR, Glickman BW, Gorelick NJ, Mirsalis JC, Martus H, Skopek TR, Thybaud V, Tindall KR, Yajima N. *In vivo* transgenic mutation assays. Environ Mol Mutagen. 2000; 35: 253–9.
15 Thybaud V, Dean S, Nohmi T, deBoer J, Douglas GR, Glickman BW, Gorelick NJ, Heddle JA, Heflich RH, Lambert I, Martis HJ, Mirsalis JC, Suzuki T, Yajima N. *In vivo* transgenic mutation assays. Mutat Res. 2003; 540: 141–51.
16 Lambert IB, Singer TM, Boucher SE, Douglas GR. Detailed review of transgenic rodent mutation assays. Mutat Res. 2005; 590: 1–280.
17 OECD, Detailed review paper on transgenic rodent mutation assays. Series on testing and assessment No. 103. OECD Environment, Health and Safety Publications; 2009. Available at: http://www.oecd.org/document/30/0,3746,en_2649_34377_1916638_1_1_1_1,00.html (accessed 28 September 2011).
18 IARC, IARC Monographs on the evaluation of the carcinogenic risk of chemicals to man: Cadmium, nickel, some epoxides, miscellaneous industrial chemicals and general considerations on volatile anesthetics. Vol. 11. Lyon: IARC Scientific Publications; 1976. p. 75–112.
19 IARC, IARC Monographs on the evaluation of the carcinogenic risks to human. Chromium, nickel and welding. Vol. 49. Lyon: IARC Scientific Publications; 1990.
20 National Toxicolgy Program. Toxicology and carcinogenesis studies of nickel subsulfide (CAS NO. 12035-72-2) in F344/N rats and B6C3F$_1$ mice (inhalation studies). Natl Toxicol Program Tech Rep Ser. 1996; 453: 5–122.
21 Sunderman FW Jr, Maenza RM. Comparisons of carcinogenicities of nickel compounds in rats. Res Commun Chem Pathol Pharmacol. 1976; 14: 319–30.
22 Yamashiro S, Gilman JPW, Hulland TJ, Abandowitz HM. Nickel sulphide-induced rhabdomyosarcoma in rats. Acta Pathol Jpn. 1980; 30: 9–22.
23 Jasmin G, Riopelle JL. Renal carcinomas and erythrocytosis in rats following intrarenal injection of nickel subsulfide. Lab Invest. 1976; 35: 71–8.
24 Sunderman FW Jr, Maenza RM, Hopfer SM, Michell JM, Allpass PR, Damjanov I. Induction of renal cancers in rats by intrarenal injection of nickel subsulfide. J Environ Pathol Toxicol. 1979; 21: 1511–27.
25 Damjanov I, Sunderman FW Jr, Michell JM, Allpass PR. Induction of testicular sarcomas in Fischer rats by intratesticular injection of nickel subsulfide. Cancer Res. 1978; 38: 268–76.
26 Albert DM, Gonder JR, Papale J, Craft JL, Dohlman HG, Reid MC, Sunderman FW Jr. Induction of ocular neoplasms in Fischer rats by intraocular injection of nickel subsulfide. Invest Ophthalmol Vis Sci. 1982; 22: 768–82.
27 Kasprzak KS, Sunderman FW Jr, Salnikow K. Nickel carcinogenesis. Mutat Res. 2003; 533: 67–97.
28 Marzin D, Vophi H. Study of mutagenicity of metal derivatives with *Salmonella typhimurium* TA102. Mutat Res. 1985; 155: 49–51.
29 Arrouijal FZ, Hildebrand HF, Vophi H, Marzin D. Genotoxic activity of nickel subsulphide α-Ni_3S_2. Mutagenesis. 1990; 6: 583–9.
30 Sunderman FW Jr. Recent research on nickel carcinogenesis. Environ Health Perspect. 1981; 40: 131–41.
31 Biggart NW, Costa M. Assessment of the uptake and mutagenicity of nickel chloride in *salmonella* tester strains. Mutat Res. 1986; 175: 209–15.
32 Magos L. Epidemiological and experimental aspects of metal carcinogenesis: physicochemical properties, kinetics, and the active species. Environ Health Perspect. 1991; 95: 157–89.
33 Hartwig A. Current aspects in metal genotoxicity. Biometals. 1995; 8: 3–11.
34 Pikalek P, Necasek J. The mutagenic activity of nickel in Corynebacterium sp. Folia Microbiologica. 1983; 28: 17–21.
35 Biedermann KA, Landolph JT. Induction of anchorage independence in human diploid foreskin fibroblasts by carcinogenic metal salts. Cancer Res. 1987; 47: 3815–23.
36 Sen P, Conway K, Costa M. Comparison of the localiza-

tion of chromosome damage induced by calcium chromate and nickel compounds. Cancer Res. 1987; 47: 2142–7.
37 Conway K, Costa M. Nonrandom chromosomal alterations in nickel-transformed Chinese hamster embryo cells. Cancer Res. 1989; 49: 6032–8.
38 Sen P, Costa M. Incidence and localization of sister chromatid exchanges induced by nickel and chromium compounds. Cancer Res. 1986; 7: 1527–33.
39 Costa M, Salnikow K, Cosentino S, Klein CB, Huang X, Zhuang Z. Molecular mechanisms of nickel carcinogenesis. Environ Health Perspect. 1994; 102 Suppl 3: 127–30.
40 Kawanishi S, Inoue S, Oikawa S, Yamashita N, Toyokuni S, Kawanishi M, Nishino K. Oxidative DNA damage in cultured cells and rat lungs by carcinogenic nickel compounds. Free Radic Biol Med. 2001; 31: 108–16.
41 Mayer C, Klein RG, Wesch H, Schmezer P. Nickel subsulfide is genotoxic *in vitro* but shows no mutagenic potential in respiratory tract tissues of BigBlue® rats and Muta Mouse *in vivo* after inhalation. Mutat Res. 1998; 420: 85–98.
42 Toyoda-Hokaiwado N, Inoue T, Masumura K, Hayashi H, Kawamura Y, Kurata Y, Takamune M, Yamada M, Sanada H, Umemura T, Nishikawa A, Nohmi T. Integration of *in vivo* genotoxicity and short-term carcinogenicity assays using F344 *gpt* delta transgenic rats: *in vivo* mutagenicity of 2,4-diaminotoluene and 2,6-diaminotoluene structural isomers. Toxicol Sci. 2010; 114, 71–8.
43 Wolfson MR, Shaffer TH. Pulmonary applications of perfluorochemical liquids: ventilation and beyond. Paediatr Respir Rev. 2005; 6: 117–27.
44 Lewis TR, Morrow PE, MaaClellan RO, Raabe OG, Kennedy GL, Schwetz BA, Goehl TJ, Roycroft JH, Chhabre RS. Establishing aerosol exposure concentrations for inhalation studies. Toxicol Appl Pharmacol. 1989; 99: 377–83.
45 Marrow PE. Possible mechanisms to explain dust overloading of the lungs. Fundum Appl Toxicol. 1988; 10: 369–84.
46 Sui H, Ohta R, Shiragiku T, Akahori A, Suzuki K, Nakajima M, Hayashi H, Masumura K, Nohmi T. Evaluation of in vivo mutagenicity by 2,4-diaminotoluene and 2,6-diaminotoluene in liver of F344 *gpt* delta transgenic rat dosed for 28 days: a collaborative study of *gpt* delta transgenic rat mutation assay. Genes Environ. 2012; 34: 25–33.
47 Dunnick JK, Elwell MR, Benson JM, Hobbs CH, Hahn FF, Halt PJ, Cheng YS, Eidson FF. Lung toxicity after 13-week inhalation exposure to nickel oxide, nickel subsulfide, or nickel sulfate hexahydrate in F344/N rats and B6C3F1 mice. Fundam Appl Toxicol. 1989; 12: 584–94.
48 Oberdörster G. Lung particle overload: implications for occupational exposure to particles. Regul Toxicol Pharmacol. 1995; 21: 123–35.
49 Pulido MD, Parrish AR. Metal-induced apoptosis: Mechanisms. Mutat Res. 2003; 533: 227–41.
50 Bottin MC, Gate L, Rihn B, Micillino JC, Nathalie M, Martin A, Nunge H, Morel G, Worbel R, Ayi-Fanou L, Champmartin C, Keith G, Binet S. Genotoxic effects of bitumen fumes in Big Blue® transgenic rat lung. Mutat Res. 2006; 596: 91–105.
51 Rihn B, Coulais C, Kauffer E, Bottin M-C, Martin P, Yvon F, Vigneron JC, Binet S, Monhoven N, Steiblen G, Keith G. Inhaled crocidolite mutagenicity in lung DNA. Environ Health Perspect. 2000; 108 Suppl 4: 341–6.
52 Micillino JC, Coulais C, Binet S, Bottin M-C, Keith G, Moulin D, Rihn BH. Lack of genotoxicity of bitumen fumes in transgenic mouse lung. Toxicology. 2002; 170: 11–20.
53 Topinka J, Loli P, Georgiadis P, Dusinska M, Hurbankova M, Kovacikova Z, Volkovova K, Kazimirova A, Barancokova M, Tatrai E, Oesterle D, Wolff T, Kyrtopoulos SA. Mutagenesis by asbestos in the lung of λ-*lacI* transgenic rats. Mutat Res. 2004; 553: 67–78.
54 Donaldson K, Brown GM, Brown DM, Bolton RE, Davis JM. Inflammation generating potential of long and short fibre amosite asbestos samples. Br J Ind Med. 1989; 46: 271–6.
55 Kamp DW, Graceffa P, Pryor WA, Weitzman SA. The role of free radicals in asbestos-induced diseases. Free Radic Biol Med. 1992; 12: 293–315.
56 Kamp DW, Weitzman SA. The molecular basis of asbestos induced lung injury. Thorax. 1999; 54: 638–52.
57 Lee YW, Klein CB, Kargacin B, Salnikow K, Kitahara J, Dowjat K, Zhitkovich A, Christie NT, Costa M. Carcinogenic nickel silences gene expression by chromatin condensation and DNA methylation: a new model for epigenetic carcinogens. Mol Cell Biol. 1995; 15: 2527–57.
58 Castranova V, Rabovsky J, Tucker JH, Miles PR. The alveolar type II epitherial cell: A multifunctional pneumocytes. Toxicol Appl Pharmacol. 1988; 93: 472–83.
59 Cairns J. Somatic stem cells and the kinetics of mutagenesis and carcinogenesis. Proc Natl Acad Sci USA. 2002; 99: 10567–70.
60 Sarasin A. An overview of the mechanisms of mutagenesis and carcinogenesis. Mutat Res. 2003; 544: 99–106.
61 Pinkerton KE, Barry BE, O'neil BJ, Raub JA, Pratt PC, Crapo JD. Morphologic changes in the lung during the lifespan of Fischer 344 rats. Am J Anatomy. 1982; 164: 155–74.
62 Jones AL, Spring-Mills E. The liver and gallbladder. In: Histology: cell and tissue biology. 5th ed. Weiss L, editor. New York: Elsevier Science Ltd; 1983. p. 707–48.
63 Cross CE, Vliet A, Louie S, Thiele JJ, Halliwell B. Oxidative stress and antioxidants at biosurfaces: plants, skin, and respiratory tract surfaces. Environ Health Perspect. 1998; 106 Suppl 5: 1241–51.
64 Noda Y, Suzuki T, Kohara A, Hasegawa A, Yotsuyanagi T, Hayashi M, Sofuni T, Yamanaka K, Okada S. *In vivo* genotoxicity evaluation of dimethylarsinic acid in Muta Mouse. Mutat Res. 2002; 513: 205–12.
65 Aoki Y, Hashimoto AH, Amanuma K, Matsumoto M, Hiyoshi K, Takano H, Masumura K, Nohmi T, Yamamoto M. Enhanced spontaneous and Benzo(*a*) pyrene-induced mutations in the lung of Nrf2-deficinet *gpt* delta mice. Cance Res. 2007; 67: 5643–8.
66 Hashimoto AH, Amanuma K, Hiyoshi K, Takano H, Masumura K, Nohmi T, Aoki Y. *In vivo* mutagenesis in

the lungs of *gpt*-delta transgenic mice treated intratracheally with 1,6-dinitropyrene. Environ Mol Mutagen. 2006; 47: 277–83.
67 Hashimoto AH, Amanuma K, Masumura K, Nohmi T, Aoki Y. *In vivo* mutagenesis caused by diesel exhaust in the tests of *gpt* delta transgenic mice. Genes Environ. 2009; 31: 1–8.

Toxicology and Applied Pharmacology 255 (2011) 297–306

Contents lists available at ScienceDirect

Toxicology and Applied Pharmacology

journal homepage: www.elsevier.com/locate/ytaap

Prediction model of potential hepatocarcinogenicity of rat hepatocarcinogens using a large-scale toxicogenomics database

Takeki Uehara [a,b,*], Yohsuke Minowa [b], Yuji Morikawa [b], Chiaki Kondo [a], Toshiyuki Maruyama [a], Ikuo Kato [a], Noriyuki Nakatsu [b], Yoshinobu Igarashi [b], Atsushi Ono [b], Hitomi Hayashi [c,d], Kunitoshi Mitsumori [c], Hiroshi Yamada [b], Yasuo Ohno [e], Tetsuro Urushidani [b,f]

[a] Drug Developmental Research Laboratories, Shionogi & Co., Ltd., 3-1-1 Futaba-cho, Toyonaka, Osaka 561-0825, Japan
[b] Toxicogenomics Informatics Project, National Institute of Biomedical Innovation, 7-6-8 Asagi, Ibaraki, Osaka 567-0085, Japan
[c] Laboratory of Veterinary Pathology, Tokyo University of Agriculture and Technology, 3-5-8 Harumi-cho, Fuchu, Tokyo 183-8509, Japan
[d] Pathogenetic Veterinary Science, United Graduate School of Veterinary Sciences, Gifu University, 1-1 Yanagido, Gifu, 501-1193 Gifu, Japan
[e] National Institute of Health Sciences, 1-18-1 Kamiyoga, Setagaya-ku, Tokyo 158-8501, Japan
[f] Department of Pathophysiology, Faculty of Pharmaceutical Sciences, Doshisha Women's College of Liberal Arts, Kodo, Kyotanabe, Kyoto 610-0395, Japan

ARTICLE INFO

Article history:
Received 7 April 2011
Revised 5 July 2011
Accepted 6 July 2011
Available online 19 July 2011

Keywords:
Toxicogenomics
Microarray
Hepatocarcinogenicity
TG-GATEs
Non-genotoxic hepatocarcinogens

ABSTRACT

The present study was performed to develop a robust gene-based prediction model for early assessment of potential hepatocarcinogenicity of chemicals in rats by using our toxicogenomics database, TG-GATEs (Genomics-Assisted Toxicity Evaluation System developed by the Toxicogenomics Project in Japan). The positive training set consisted of high- or middle-dose groups that received 6 different non-genotoxic hepatocarcinogens during a 28-day period. The negative training set consisted of high- or middle-dose groups of 54 non-carcinogens. Support vector machine combined with wrapper-type gene selection algorithms was used for modeling. Consequently, our best classifier yielded prediction accuracies for hepatocarcinogenicity of 99% sensitivity and 97% specificity in the training data set, and false positive prediction was almost completely eliminated. Pathway analysis of feature genes revealed that the mitogen-activated protein kinase p38- and phosphatidylinositol-3-kinase-centered interactome and the v-myc myelocytomatosis viral oncogene homolog-centered interactome were the 2 most significant networks. The usefulness and robustness of our predictor were further confirmed in an independent validation data set obtained from the public database. Interestingly, similar positive predictions were obtained in several genotoxic hepatocarcinogens as well as non-genotoxic hepatocarcinogens. These results indicate that the expression profiles of our newly selected candidate biomarker genes might be common characteristics in the early stage of carcinogenesis for both genotoxic and non-genotoxic carcinogens in the rat liver. Our toxicogenomic model might be useful for the prospective screening of hepatocarcinogenicity of compounds and prioritization of compounds for carcinogenicity testing.

Introduction

Carcinogenicity is one of the most serious side effects associated with new drug development. Thus, it is especially important for pharmaceutical companies to know as much as possible about the eventual carcinogenic properties of new drugs, even in the early stages of drug development. However, the current "gold standard" for carcinogenicity testing is a bioassay in which mice and rats are treated with a target compound for their entire 2-year lifespan. This carcinogenicity testing cannot be performed in the early stage of drug development because it is time-consuming and expensive and it requires the use of many animals and large amounts of chemicals. Additionally, while this assay provides evidence of carcinogenicity of the target chemicals in rodents, it provides only limited mechanistic information about carcinogenesis. Thus, the current strategy of a 2-year bioassay to evaluate in vivo carcinogenicity is not satisfactory. It should be replaced with better test systems that are cheaper and faster, use fewer animals, and provide the appropriate sensitivity and specificity desired for a screen of carcinogenic potential.

Toxicogenomics has been expected as a powerful approach for elucidating mechanisms underlying toxicological endpoints and a useful strategy for the early detection of potential chemical toxicity (Battershill, 2005; Heinloth et al., 2004; Irwin et al., 2004; Kiyosawa et al., 2009; Searfoss et al., 2005). Important scientific breakthroughs have been achieved by applying toxicogenomics to the early detection of chemical carcinogenicity in vivo. Studies have focused on hepatocarcinogenicity because the liver is the most common target organ for carcinogenesis. Kramer et al. (2004) studied microarray-derived comprehensive gene

* Corresponding author at: Developmental Research Laboratories, Shionogi & Co., Ltd., 3-1-1 Futaba-cho, Toyonaka, Osaka 561-0825, Japan. Fax: +81 6 6332 6385.
E-mail address: takeki.uehara@shionogi.co.jp (T. Uehara).

0041-008X/$ – see front matter © 2011 Elsevier Inc. All rights reserved.
doi:10.1016/j.taap.2011.07.001

expression data from the livers of rats treated with 10 non-genotoxic hepatocarcinogens and determined that the expression level of NAD(P)H P450 reductase was positively correlated with hepatocarcinogenicity and the expression level of transforming growth factor-β clone 22 was negatively correlated with hepatocarcinogenicity. Nie et al. (2006) demonstrated that 6 biomarker genes predict the carcinogenic potential of non-genotoxic hepatocarcinogens with a prediction accuracy of 88.5% by using expression data from the livers of rats treated with a single dose of 24 non-genotoxic chemicals and 28 non-hepatocarcinogens. Nakayama et al. (2006) successfully separated several isomers with or without hepatocarcinogenicity based on the expression profiles of selected genes, and they identified characteristic gene expression changes in hepatocarcinogenic isomers after up to 28 days of repeated dosing. Ellinger-Ziegelbauer et al. (2008) constructed support vector machine (SVM) prediction models by using gene expression data from rats treated for up to 14 days with 13 different chemicals for the training set and rats treated with 16 independent chemicals for the validation set; the resulting prediction models differentiated between genotoxic hepatocarcinogens, non-genotoxic hepatocarcinogens and non-hepatocarcinogens with up to 88% classification accuracy. Fielden et al. (2007) analyzed hepatic gene expression in rats treated with 25 non-genotoxic hepatocarcinogens and 75 non-hepatocarcinogens for 1 to 7 days. They constructed a SVM model consisting of 37 probes that yielded prediction accuracies for carcinogenicity with 86% specificity and 81% sensitivity. These researchers successfully constructed gene-based prediction models from data obtained from up to 1 month of repeated dosing. In contrast, Auerbach et al. (2010) recently demonstrated further evidence that the dosing period is an important factor in the construction of highly accurate prediction models based on toxicogenomics-derived gene expression profiles, especially in the case of weakly carcinogenic compounds. They concluded that a 90-day exposure period is needed to detect gene expression changes specifically related to carcinogenic compounds.

In Japan, the Toxicogenomics Project (TGP) has established a large-scale toxicogenomics database known as TG-GATEs (Genomics-Assisted Toxicity Evaluation System developed by the Toxicogenomics Project in Japan) (Uehara et al., 2010; Urushidani, 2010). In this project, rats were exposed to 3 different doses of 150 compounds for a period ranging from 1 to 28 days; the gene expression in the livers and kidneys of these animals at 8 different time points was comprehensively analyzed using microarrays. We have used this database to identify several different types of biomarker genes and construct prediction models for hepatotoxicity and nephrotoxicity (Gao et al., 2010; Hirode et al., 2008; Kondo et al., 2009; Uehara et al., 2010). Regarding hepatocarcinogenicity, we previously tried to build a gene-based predictor of non-genotoxic hepatocarcinogenicity in rats (Uehara et al., 2008). Consequently, we have successfully built a model, consisting of 112 probes, for the early detection of hepatocarcinogenesis based on gene expression changes that are commonly induced by compounds with hepatocarcinogenicity in rats. However, since this model was trained to achieve early and sensitive detection of potential carcinogenicity after a single exposure to a compound, false positive predictions occurred in some non-carcinogenic hepatotoxins. Moreover, a limited number of compounds were used for training of the model in the study since our database was under construction. In an effort to make high-quality predictive models based on gene expression data, a fairly extensive data set of several compounds with multiple time points and multiple dose levels is required. Now, our large-scale toxicogenomics database has been completed, and microarray data for all 150 compounds are available. In this research, we hypothesized that our large-scale toxicogenomics database might lead to the construction of a more robust and accurate prediction model of hepatocarcinogenicity in rats. By taking into account the findings of the latest work by Auerbach et al. (2010), we have trained a classifier by using data from our longest dosing period (28 days) to decrease the percentage of false-positive predictions. Consequently, our new SVM-based classifier yielded prediction accuracies for hepatocarcinogenicity with 99% sensitivity and 97% specificity in a training data set, and false-positive predictions were almost completely eliminated. The usefulness and robustness of our predictor were further confirmed in an independent validation data set obtained from a public database. Interestingly, similar positive predictions were obtained for several genotoxic hepatocarcinogens as well as non-genotoxic hepatocarcinogens. In the present report, we provide reliable candidate gene biomarkers in the early stages of the hepatocarcinogenesis that are predictive for both genotoxic and non-genotoxic hepatocarcinogens. Our present toxicogenomic model might be useful to reduce the dependence on 2-year rodent bioassays by instead using a short-term repeated dosing study.

Materials and methods

Animals and experimental design. Five-week-old male Sprague–Dawley rats were obtained from Charles River Japan, Inc. (Kanagawa, Japan). After a 7-day quarantine and acclimatization period, the 6-week-old animals were assigned to dosage groups (5 rats per group) by using a computerized stratified random grouping method based on individual body weight. The animals were individually housed in stainless-steel cages in an animal room that was lighted for 12 h (7:00–19:00) daily, ventilated with an air-exchange rate of 15 times per hour, and maintained at 21 °C–25 °C with a relative humidity of 40%–70%. Each animal was allowed free access to water and a pellet diet (CRF-1, sterilized by radiation, Oriental Yeast Co., Ltd., Tokyo, Japan).

The compounds used in this study are summarized in Table 1 (for detailed experimental conditions, see Supplemental Table 1). A total of 150 compounds were used for training and testing of models. The training data set consisted of 6 positive compounds (necrogenic hepatocarcinogens with no evidence of genotoxicity, namely non-genotoxic hepatocarcinogens) and 54 negative compounds (non-hepatocarcinogens), and the test data set consisted of remaining 90 compounds (for more detailed information, see Supplemental Table 2). According to the standard protocol in our project (Uehara et al., 2010), 5 rats per group were treated with these compounds at 3 different dose levels (low: L, middle: M, and high: H). The maximum tolerated dose of each compound, which was estimated from a preliminary 7-day repeated dosing study, was chosen as the highest dose level. For single-dose studies, rats were euthanized at 3, 6, 9 and 24 h after dosing. For repeated dose studies, the animals were treated daily for 3, 7, 14 and 28 days and euthanized 24 h after the last dosing (4, 8, 15 and 29D). The animals were euthanized by exsanguination from the abdominal aorta under ether anesthesia, and liver samples were collected from the left lateral lobe of the liver immediately after the animals were euthanized. The experimental protocols were carefully reviewed and approved by the Ethics Review Committee for Animal Experimentation of the National Institute of Health Sciences.

RNA extraction and microarray analysis. An aliquot of the sample (about 30 mg) for microarray analysis was obtained from the left lateral lobe of the liver in each animal immediately after the animals were euthanized. The sample was kept in RNAlater® (Ambion, Austin, TX, USA) overnight at 4 °C and then frozen at −80 °C until use. Liver samples were homogenized with buffer RLT supplied in the RNeasy Mini Kit (Qiagen, Valencia, CA, USA), and total RNA was isolated according to the manufacturer's instructions.

Microarray analysis was conducted on 3 of 5 samples for each group by using Affymetrix Rat Genome 230 2.0 arrays (Affymetrix, Santa Clara, CA, USA). The procedure was basically conducted according to the manufacturer's instructions as previously reported (Uehara et al., 2010). The digital image files were preprocessed by Affymetrix Microarray Analysis Suite version 5.0 (MAS5.0). The expression signal values were scaled by the median of each chip sample. The normalized data sets were then converted into the log-ratio of base 2 to the means of the

Table 1
Compounds and carcinogenicity definitions used in this study.

Compound class	Compound name
Training set (positive)	
Non-genotoxic hepatocarcinogen (hepatotoxic oxidative stressor)	Carbon tetrachloride (CCL4), ethionine (ET), thioacetamide (TAA), methapyrilene (MP), coumarin (CMA), monocrotaline (MCT)
Training set (negative)	
Non-hepatocarcinogen	Acetaminophen (APAP), naphthyl isothiocyanate (ANIT), allyl alcohol (AA), theophylline (TEO), trimethadione (TMD), naproxen (NPX), methotrexate (MTX), aspirin (ASA), labetalol (LBT), ketoconazole (KC), tetracycline (TC), metformin (MFM), methyldopa (MDP), vitamin A (VA), chlorpropamide (CPP), nicotinic acid (NIC), famotidine (FAM), ranitidine (RAN), diltiazem (DIL), captopril (CAP), enalapril (ENA), mexiletine (MEX), meloxicam (MLX), lornoxicam (LNX), cyclosporine A (CSA), isoniazid (INAH), phenylbutazone (PhB), nitrofurantoin (NFT), propylthiouracil (PTU), amiodarone (AM), cimetidine (CIM), flutamide (FT), methimazole (MYZ), iproniazid (IPA), chloramphenicol (CMP), furosemide (FUR), chlorpheniramine (CHL), caffeine (CAF), sulpiride (SLP), simvastatin (SST), chlormadinone (CLM), carboplatin (CBP), bucetin (BCT), perhexiline (PH), pemoline (PML), ibuprofen (IBU), erythromycin ethylsuccinate (EME), nifedipine (NIF), sulindac (SUL), disopyramide (DIS), disulfiram (DSF), tolbutamide (TLB), acarbose (ACA), ajmaline (AJM)
Test set	
Genotoxic hepatocarcinogen	Lomustine (LS), acetamidofluorene (AAF), nitrosodiethylamine (DEN)
Non-genotoxic hepatocarcinogen (enzyme inducer)	Phenobarbital (PB), carbamazepine (CBZ), phenytoin (PHE), rifampicin (RIF), hexachlorobenzene (HCB), sulfasalazine (SS)
Non-genotoxic hepatocarcinogen (peroxisome proliferator)	Clofibrate (CFB), WY-14643 (WY), gemfibrozil (GFZ), fenofibrate (FFB)
Non-genotoxic hepatocarcinogen (hormonal modulator)	Ethinylestradiol (EE)
Non-hepatocarcinogen/unknown (non-genotoxicant)	Ethionamide (ETH), indomethacin (IM), bromobenzene (BBZ), ethambutol (EBU), colchicine (COL), clomipramine (CPM), puromycin aminonucleoside (PAN), methyltestosterone (MTS), valproic acid (VPA), chlorpromazine (CPZ), diclofenac (DFNa), benzbromarone (BBr), allopurinol (APL), fluphenazine (FP), thioridazine (TRZ), adapin (ADP), glibenclamide (GBC), chlormezanone (CMN), moxisylyte (MXS), imipramine (IMI), amitriptyline (AMT), hydroxyzine (HYZ), quinidine (QND), mefenamic acid (MEF), tiopronin (TIO), acetazolamide (ACZ), promethazine (PMZ), dantrolene (DTL), triazolam (TZM), terbinafine (TBF), danazol (DNZ), bendazac (BDZ), benziodarone (BZD), bromoethanamine (BEA), nimesulide (NIM), phenylanthranilic acid (NPAA), cephalothin (CLT), ticlopidine (TCP), gentamicin (GMC), vancomycin (VMC), omeprazole (OPZ), diazepam (DZP), haloperidol (HPL), griseofulvin (GF), tamoxifen (TMX), tannic acid (TAN), triamterene (TRI), ethanol (ETN), ciprofloxacin (CPX), tacrine (TAC), nitrofurazone (NFZ), papaverine (PAP), penicillamine (PEN), azathioprine (AZP), doxorubicin (DOX), cyclophosphamide (CPA), etoposide (ETP), cisplatin (CSP), phenacetin (PCT)
Unknown	K01, K02, K03, K04, K05, K06, K07, K08, K09, K10, K11, K12, K13, K14, K15, K16, K17

K01 to K17 were compounds synthesized in member companies.

corresponding control groups. Raw microarray data (CEL files) are available in Open TG-GATEs (http://toxico.nibio.go.jp/).

Gene selection and supervised classification. Among a total of 150 compounds in our database, we have selected 6 compounds consisting of carbon tetrachloride, ethionine, thioacetamide, methapyrilene, coumarin and monocrotaline, as positive training compounds for modeling, which are non-genotoxic hepatocarcinogens with hepatocellular necrosis/degeneration in histopathology following multiple dosing for up to 28 days in our experimental condition. Individual histopathological data of all compounds are available (http://toxico.nibio.go.jp/datalist.html). High-dose 29D groups treated with these compounds were used for the positive training data set, with the exception for monocrotaline; the middle-dose group of monocrotaline at 29D was included in the positive training set because all animals in the high-dose group were dead at 29D in the current experimental condition. High- or middle-dose groups at all time points (3 to 24H for single-dose studies, 4 to 29D for repeated-dose studies) of randomly selected 54 non-hepatocarcinogens were selected as the negative training data set. To exclude genes being transiently regulated by the treatment of non-carcinogenic compounds, data obtained from all time points were used as the negative training set. The remaining compounds were used as the independent test set as follows: (i) genotoxic hepatocarcinogens; (ii) non-genotoxic hepatocarcinogens whose carcinogenic mechanisms are thought to be related to hepatic enzyme induction, peroxisomal proliferation and hormonal modulation; and (iii) non-hepatocarcinogens (for more detailed information, see Supplemental Table 2).

SVM combined with wrapper-type gene selection algorithms was used to build a prediction model, as previously reported (Kondo et al., 2009). First, the probes that were judged as absent in all samples of the training data set using MAS5.0 P/A-call were excluded. Next, the following 3 statistical parameters were calculated for each probe: (i) fold change of gene expression between positive and negative training data sets; (ii) Mann–Whitney U value; (iii) confident margin of SVM classifier (normal margin corrected by classification accuracy). The probes were filtered by following criteria: (i) fold change >2 or <0.5; (ii) p-value <0.01; and (iii) confident margin >0.05. Then, the combined gene ranking based on the 3 parameters was calculated by using a layer ranking algorithm (Chen et al., 2007). To estimate the performance of our classifier, 5-fold cross-validation was executed as described in our previous report (Kondo et al., 2009). Finally, 9 of the 82 top-ranked probes (7 genes) were selected to maximize the classification accuracy and the area under the curve (AUC) of the receiver operating characteristic curve (ROC).

Ingenuity pathways analysis. The 82 top-ranked probes were analyzed by using Ingenuity Pathways Analysis software (v. 7.1; Ingenuity Systems, Redwood City, CA) to determine the biological networks that were enriched in selected feature genes.

Independent validation of our classifier by using an external data set from NEDO. An external microarray data set from the NEDO project, another toxicogenomics consortium in Japan, was used for independent validation of our classifier (Matsumoto et al., 2009). In this project, the NEDO-ToxArray III consists of 6709 genes, and hepatic gene expression data was comprehensively obtained from F344 rats treated with 88 compounds for up to 28 days. All of the microarray data are available in the public microarray database of Gene Expression Omnibus (GEO). SVM modeling and principal component analysis (PCA) were performed by using the expression data at 3 different time points (4, 15 and 29D).

Predictions using published biomarker genes. For comparison of prediction accuracy with previously published models, we built

SVM models with our training data set by using published gene lists and then compared the prediction performance of all models (Auerbach et al., 2010; Ellinger-Ziegelbauer et al., 2008; Fielden et al., 2007; Nakayama et al., 2006; Uehara et al., 2008). To estimate the performance of each model, 5-fold cross-validation was executed using the training data set.

Results

Gene selection and supervised classification. We trained a binary classifier by using an SVM algorithm combined with wrapper-type gene selection to construct a statistically reliable model without over-fitting to the profiles of training samples according to our previous report with minor modifications (Kondo et al., 2009). By applying statistical analysis for feature selection, 82 probes passed current statistical criteria, and these top-ranked probes are summarized in Supplemental Table 3. 1 to 82 of the top-ranked probes were used to construct the classifiers with further feature selection. A ROC curve and its AUC are plotted in Fig. 1. Although there were no big differences in the prediction accuracy of each classifier, a classifier consisting of 9 probes (7 genes; Table 2) achieved the best classification accuracy under the 5-fold cross-validation. The sensitivity and specificity of the prediction of the optimized classifier was 99% and 97%, respectively.

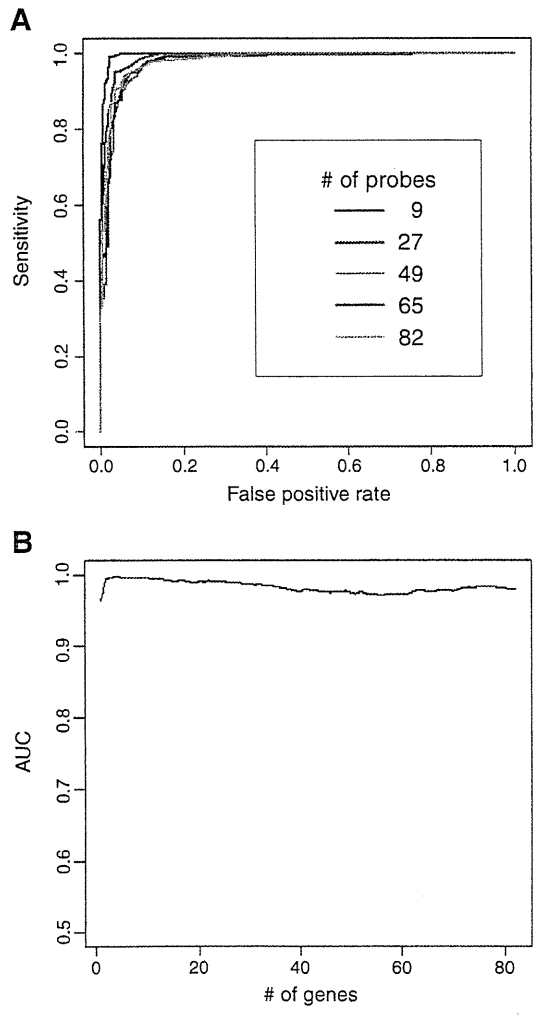

Fig. 1. Receiver operating characteristic analysis of prediction models. ROC curve (A) and area under the ROC curve (B) of prediction models are plotted. A model consisting of 9 probes was selected as the best model in our training data set.

Table 2
The 9 top-ranked probes in the optimized model.

Affymetrix probe ID	Gene title	Gene abbreviation	GO biological process (selected)
1370583_s_at	ATP-binding cassette, sub-family B (MDR/TAP), member 1A/1B	*Abcb1a/1b*	Nucleotide binding/transporter activity/protein binding/ATP binding/ATPase activity/drug transporter activity/hydrolase activity/nucleoside-triphosphatase activity
1395737_at /1374198_at	Cd276 molecule	*Cd276*	Receptor binding/protein binding
1367787_at	Islet cell autoantigen 1	*Ica1*	Protein binding/protein domain specific binding
1379419_at	Transmembrane protein 184C	*Tmem184c*	Unknown
1379262_at	Acyl-CoA thioesterase 9	*Acot9*	Unknown
1383401_at	Testis derived transcript	*Tes*	Zinc ion binding/metal ion binding
1375719_s_at/1373102_at	Cadherin 13	*Cdh13*	Calcium ion binding/protein binding/low-density lipoprotein binding/protein homodimerization activity/cadherin binding/adiponectin binding

Gene expression profiles of selected feature genes. Fig. 2 shows a heat map of the selected 9 probes and all 82 top-ranked probes. Among the 82 probes, 44 probes were upregulated, and 38 probes were downregulated in positive training compounds. All 9 probes involved in the optimized model were upregulated in positive training compounds. The extent of upregulation of genes in positive compounds was clearly higher than that in negative compounds and changed in a time- and dose-dependent manner (Fig. 3).

Ingenuity pathways analysis. To further characterize the biological significance of alterations in gene expression, functional pathway analysis was performed by using the 82 selected probes. The mitogen-activated protein kinase p38 (*p38 Mapk*)- and phosphatidylinositol-3-kinase (*Pl3k*)-centered interactome (Fig. 4A) and the v-myc myelocytomatosis viral oncogene homolog (*Myc*)-centered interactome (Fig. 4B) were the 2 most significant networks. Among 9 probes (7 genes) of the best classifier, the following 5 genes were involved in these networks: ATP-binding cassette, sub-family B (MDR/TAP), member 1A/B (*Abcb1a/b*), Cd276 molecule (*Cd276*), islet cell autoantigen 1 (*Ica1*), testis-derived transcript (*Tes*), and cadherin 13 (*Cdh13*).

Prediction results of all compounds. The SVM classification scores of all 150 compounds are summarized in Supplemental Table 2. All 3 dose groups of 90 test compounds that had not been used as the training set and the remaining groups of the 60 training compounds were used as a test data set for external validation of the classifier. The classifier predicted the following samples as positive: thioacetamide (H: 8D and 15D; M: 29D), methapyrilene (H: 8D and 15D), carbon tetrachloride (M: 29D) and monocrotaline (H: 15D). As expected, positive predictions for several hepatocarcinogens were observed only after long-term repeated dosing. There were no positive predictions in the low-dose groups of these positive-training compounds. Among the

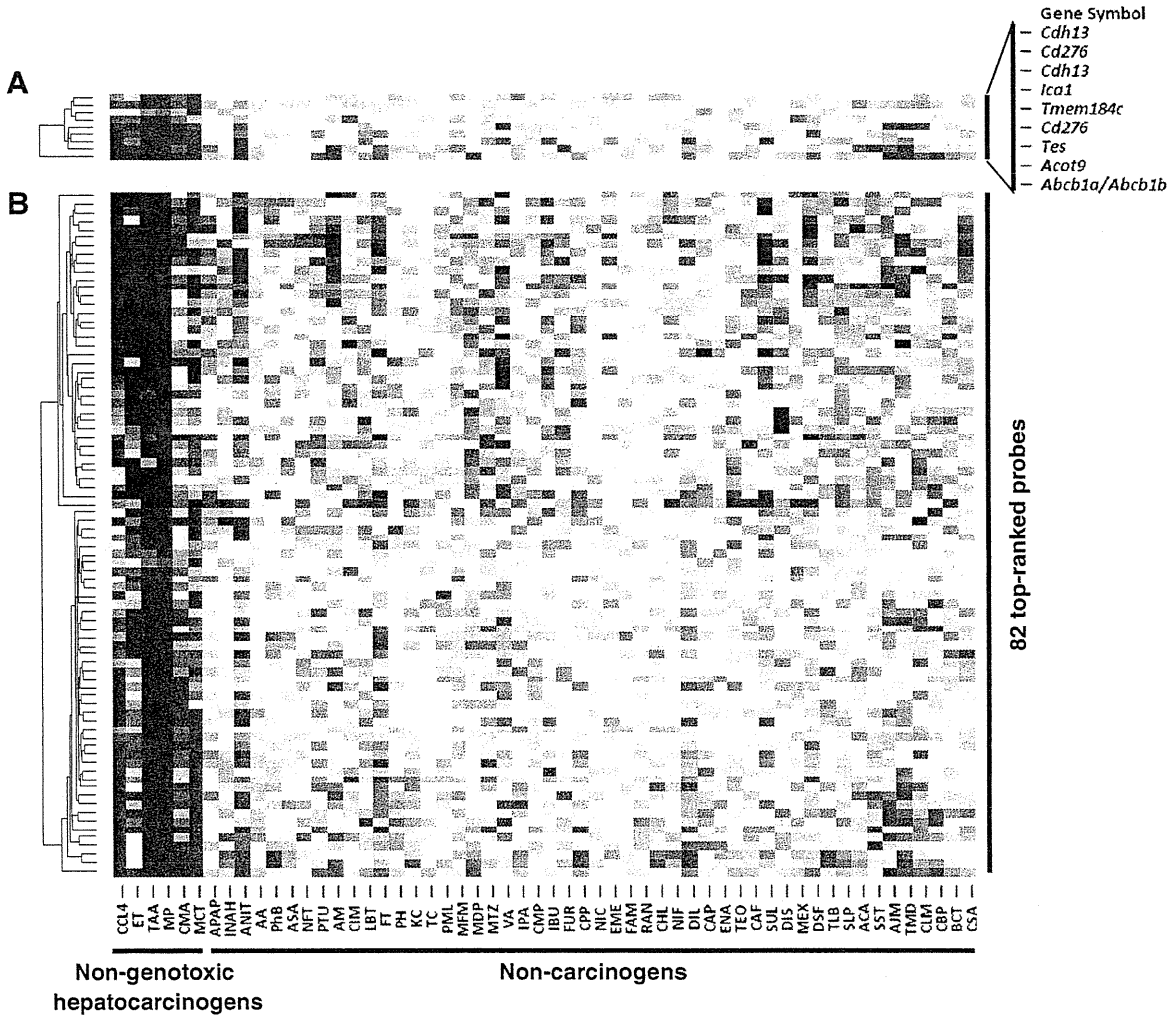

Fig. 2. Hierarchical clustering analysis of expression changes of selected feature genes. Gene expression changes of the 9 (A) and 82 top-ranked probes (B) were analyzed by hierarchical clustering. Clustering method: UPGMA (unweighted average); similarity measure: Euclidean distance; ordering function: average value. Heat map shows log-ratio of base 2 to the means of the corresponding control groups (red: 5-fold higher, blue: -5-fold lower expression of log 2 ratio). Symbols of selected genes are shown on the right side of the heat map.

genotoxins, lomustine (H: 29D), acetamidofluorene (L, M and H: 15 and 29D) and nitrosodiethylamine (M: 29D and H: 8 and 15D), for which the target of carcinogenicity is the liver, were correctly predicted as positive. Several genotoxic compounds that have potential to elicit cancer in other target organs, such as cyclophosphamide, etoposide, cisplatin and carboplatin, colchicine, phenacetin and doxorubicin, were predicted as negative at all time points of the 3 dose groups. Non-genotoxic hepatocarcinogens, including enzyme inducers (phenobarbital, carbamazepine, phenytoin, rifampicin, hexachlorobenzene and sulfasalazine), peroxisome proliferators (clofibrate, Wy-14643, gemfibrozil and fenofibrate) and hormonal modulators (ethinylestradiol), were classified as negative in all groups. The priority focus on this study was to build a prediction model with improved false-positive classification of non-hepatocarcinogens reflecting temporal gene expression changes at early time points after single or short-term repeated dosing. Among the 46 compounds in the negative/unknown test set, almost all compounds were classified as negative except for 2 compounds that were falsely classified as positive, ethionamide (H: 24H, 4D, and 15D; M: 24H) and etambutol (H: 8D).

Further independent validation of the optimized predictor. Since interlaboratory difference is an important issue in the field of toxicogenomics research (Fielden et al., 2008), a further independent validation was performed by using microarray data obtained by independent laboratories. In the present study, we used an external data set obtained in the NEDO project for further validation (Matsumoto et al., 2009). The NEDO study used custom microarrays consisting of 6709 probes, and gene expression data was comprehensively obtained from the livers of rats treated with several compounds for up to 28 days. Among their data set, we used following 14 compounds commonly involved in our data set: carbon tetrachloride, ethionine, thioacetamide, methapyrilene and nitrosodiethylamine (positive test set), and phenobarbital, phenytoin, hexachlorobenzene, clofibrate, ethinylestradiol, indomethacin, acetaminophen, aspirin and tannic acid (negative test set). For the purpose of a comprehensive comparison, we used 82 top-ranked probes for this analysis. Due to differences in the microarray platform, only 53 out of 82 probes were shared by both microarray platforms. By using the gene expression data for 53 probes, a SVM classifier was built without further feature selection using our training data set and then analyzed prediction accuracy of these test chemicals. As a result, all hepatocarcinogens included in the test data set were correctly predicted as positive regardless of using microarray data obtained by the different platform in independent laboratories. The overall sensitivity and specificity of the prediction by this classifier consisting of 53 probes was 100% and 89%, respectively (Supplemental Table 4).

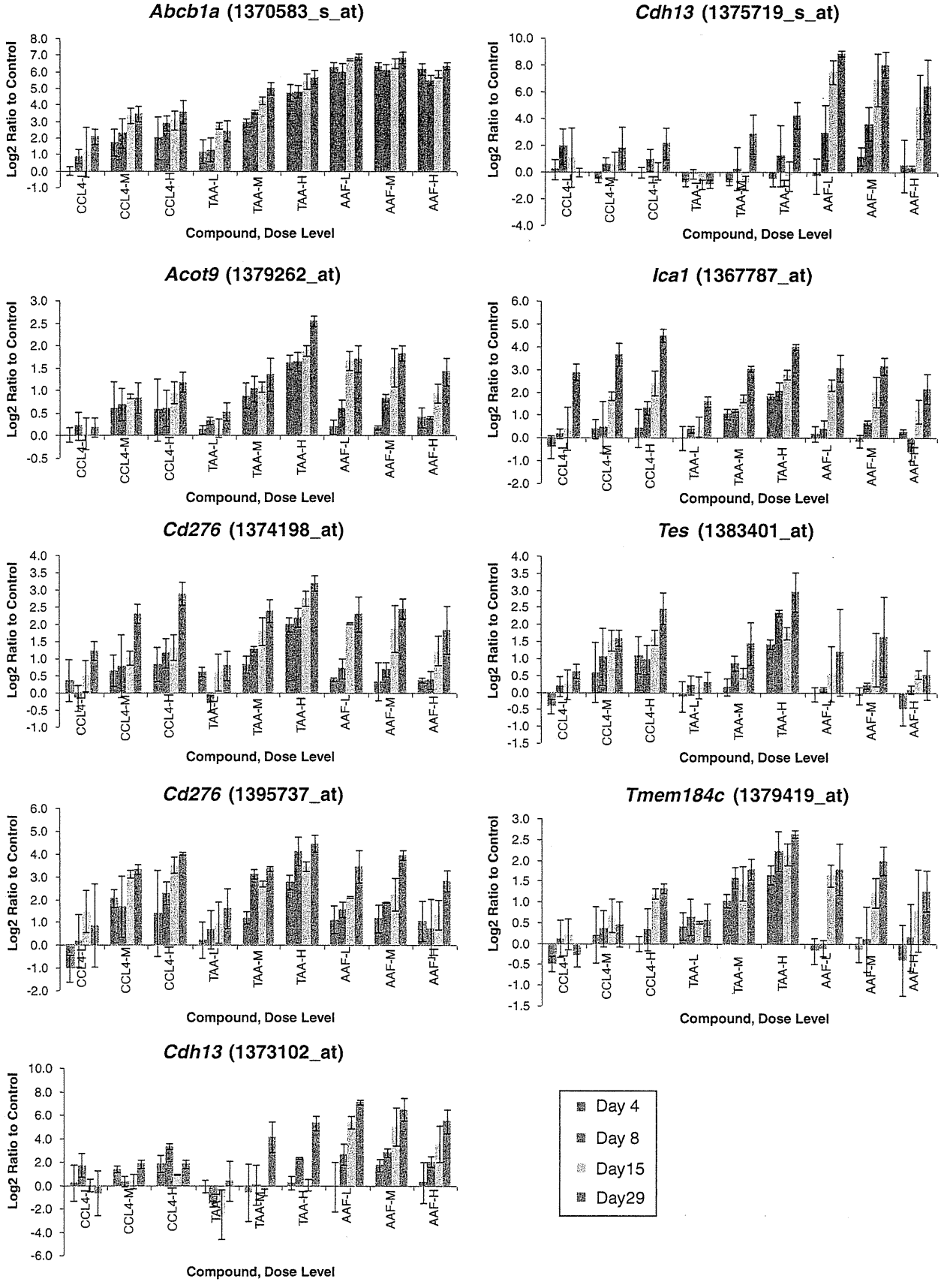

Fig. 3. Effect of dose and exposure duration on the expression of candidate biomarker genes for hepatocarcinogenesis. Log-ratio of base 2 to the means of the corresponding control groups with standard deviation are shown in 3 representative hepatocarcinogens, carbon tetrachloride, thioacetamide and acetamidofluorene.

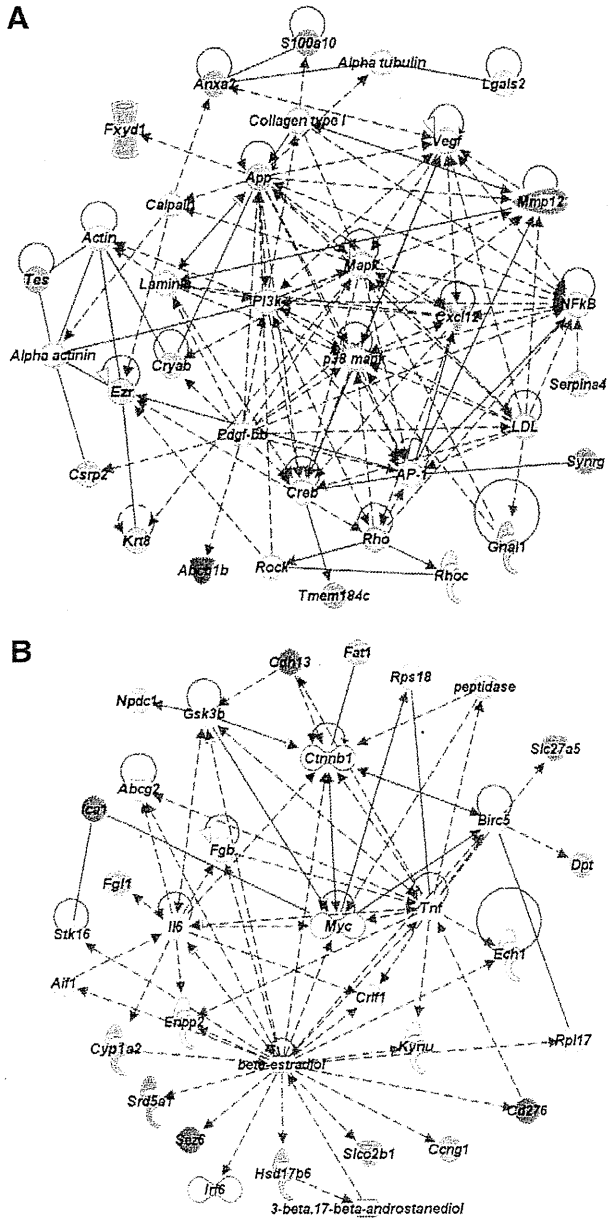

Fig. 4. Molecular networks representing selected feature genes. *p38 Mapk*- (A) and *Myc*-centered interactomes (B) were selected as significant network in the selected 82 genes. Red and green represent molecules upregulated or downregulated in positive compounds compared to negative compounds, respectively. Molecules incorporated into the network are shown in white. Ellipse, square, triangle, trapezoid, lozenge and circle represent transcription regulator, cytokine, kinase, transporter, enzyme and other molecules, respectively. Arrows connecting molecules indicate one molecule acts on another, and lines indicate one molecule binds to another. Dashed arrows or lines indicate indirect interactions of 2 molecules.

Furthermore, unsupervised analysis, PCA, was also performed based on the expression profiles of 53 probes in all of the NEDO data set. The scores of the first and second principal components (PC1 and PC2) at 4, 15 and 29D were separately plotted in Fig. 5. Several genotoxic hepatocarcinogens, such as nitrosodiethylamine, N-nitrosomorpholine, 2-nitropropane, furan and N-nitrosopiperidine, which show positive findings in in vitro genotoxicity assays and in vivo carcinogenicity assays in rats, were separately plotted from non-hepatocarcinogens toward the PC1 direction. In addition, non-genotoxic hepatocarcinogens, methapyrilene, thioacetamide and carbon tetrachloride, which are also included in our data set, showed clear separations in the PC1 direction. In almost all of these compounds, a distinct separation was observed in the data set after long-term repeated dosing.

Predictions using published biomarker genes. ROC curves of all models are plotted in Fig. 6. Although there was no large overlap of genes among the models, all models showed high prediction performance in our data set. Among all models, our new model achieved the best classification accuracy under the 5-fold cross-validation (Table 3).

Discussion

The goal of the present study was to develop a robust toxicogenomic model for the early assessment of potential hepatocarcinogenicity of chemicals based on gene expression changes stored in our toxicogenomics database, TG-GATEs. Carcinogenesis occurs via multiple mechanisms. Based on the properties of DNA damage, carcinogens are classified as genotoxins or non-genotoxins. Genotoxic carcinogens induce direct DNA damage, that is detectable by in vitro genotoxicity assays (e.g., Ames test and chromosomal aberration assays) and in vivo micronucleus test. Non-genotoxic carcinogens act through various modes of action that do not involve direct DNA damage (e.g., hepatocellular necrosis and regenerative proliferation, xenobiotic receptor agonists, peroxisome proliferation, or hormonal-mediated processes). Although it would be useful to detect the potential hepatocarcinogenicity of these different classes of non-genotoxic hepatocarcinogens by a single model, it is generally believed that a mechanism-based approach would be a promising strategy for robust toxicogenomic modeling since different classes of compounds generally show different gene expression profiles. In the present study, we have tried to establish reliable candidate gene biomarkers to assess the potential risks of hepatocarcinogenicity in the early stage of drug development with a particular focus on liver necrogenic compounds. Consequently, we have successfully identified robust biomarker genes specifically upregulated in necrogenic compounds with hepatocarcinogenicity. In contrast, no positive predictions were observed in the other class of non-genotoxic hepatocarcinogens involved in hepatic enzyme inducers, peroxisome proliferators and hormonal modulators. Therefore, these characteristics of prediction profile might help to elucidate the mechanisms of action involved in non-genotoxic hepatocarcinogenesis.

In contrast to our previous classifier (Uehara et al., 2008), our current model successfully achieved robust detection of non-genotoxic hepatocarcinogenicity of compounds by using hepatic gene expression data after 28 days of repeated dosing. There were some differences in the prediction properties of these 2 models. Namely, the current model enables us to detect robust gene expression changes possibly related to hepatocarcinogenic process following chronic doses in contrast to the previous model, which is useful to detect early temporal signals after a single dose as well as repeated doses; therefore, the combined use of both models for comprehensive judgment is thought to be the best strategy for sensitive and robust detection of hepatocarcinogenicity in short-term repeated dosing studies.

Interestingly, our current classifier as well as the previous classifier (data not shown) provided positive prediction results for not only non-genotoxic hepatocarcinogens but genotoxic hepatocarcinogens as well. This observation was further confirmed by the external test data set from the NEDO project (Matsumoto et al., 2009). It is generally believed that genotoxic compounds directly induce DNA damage by themselves or their reactive metabolites and that sufficient initiation is achieved after a single dose or short-term repeated doses due to the strong potency of their genotoxic stimulus. In contrast, non-genotoxic carcinogens generally require repeated dosing for sufficient initiation. Although the mechanisms involved in hepatocarcinogenic process are not the same between genotoxic and non-genotoxic hepatocarcinogens, our selected genes showed similar

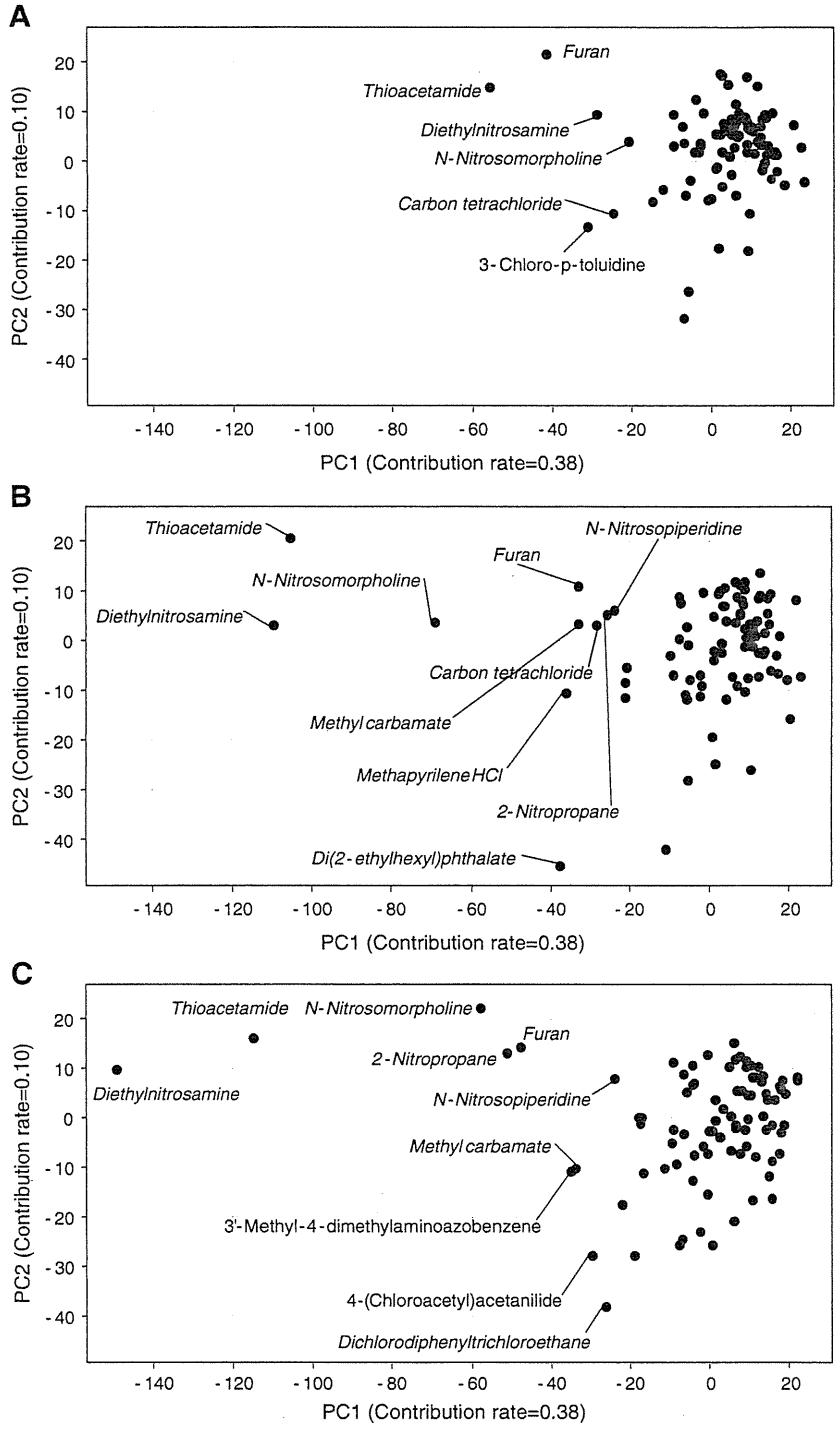

Fig. 5. Principal component analysis in independent validation. An external microarray data set obtained from the NEDO project was used for independent validation of our model. PCA was performed on all compounds by using the expression data at 3 different time points of 4 (A), 15 (B) and 29D (C). Italic font indicates hepatocarcinogens. Several hepatocarcinogens were separated from other chemicals including non-carcinogens toward the direction of PC1.

expression profiles after repeated dosing. Our results indicate that the expression profiles of our newly selected candidate biomarker genes might be common characteristics in the early stage of hepatocarcinogenic process, regardless of the type of carcinogens.

Among the test compounds, ethionamide and etambutol showed positive predictions in the current model, although there is no direct evidence supporting the hepatocarcinogenicity of these compounds in rodents. In our experiments, repeated doses of ethionamide caused anisokaryosis of centrilobular hepatocytes. In the etambutol-treated liver, karyomegaly was observed in hepatocytes with distinct nucleoli. Although it is hard to conclude that these morphological changes in the nucleus of hepatocytes are directly connected to hepatocarcinogenicity, these morphological changes might be early indicative changes of hepatocarcinogenesis and reflect nuclear DNA damage caused by these compounds. Thus, gene expression changes after further long-term repeated dosing as well as a 2-year bioassay study would be of particular

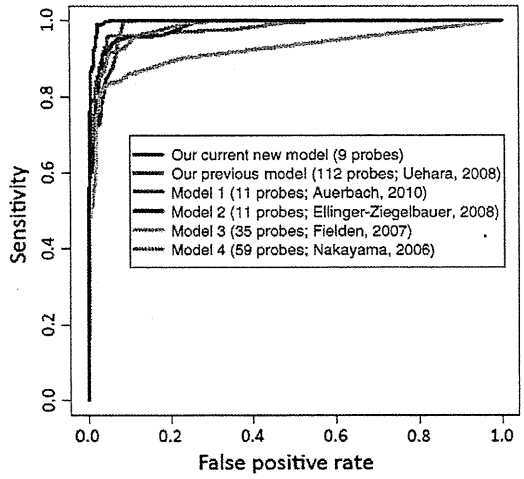

Fig. 6. Receiver operating characteristic analysis of previously published prediction models. ROC curves of prediction models are plotted. Our current new model: prediction results obtained by the best model consisting of 9 probes are shown. Model 1: a model consisting of 11 probes in the 90-day optimal-model, which showed the best prediction performance in our data set among their models, was used for this analysis. Model 2: among their models, commonly selected 101 probes were used for modeling. Models 3 and 4: 35 and 56 probes were used for modeling. Lists of genes used for each modeling are shown in Supplemental Table 5.

interest to determine the carcinogenic potentials of these compounds as well as to confirm the biological significance of these gene expression changes.

This study also provided the novel biological information that modulation of *p38 Mapk*- and *Myc*-centered networks is a common characteristic of gene expression in the early stage of hepatocarcinogenesis. There is increasing evidence that *p38 Mapk*, which is a stress-activated kinase, also participates in cell-cycle regulation, functioning as a suppressor of cell proliferation and tumorigenesis (Campbell et al., 2011). *p38* plays essential roles in modulating chronic inflammation-related cytokine expression, such as tumor necrosis factor α, interleukin 6 and 12, which might act as promoters of cancer growth and progression (Karin et al., 2006; Kumar et al., 2003; Naugler et al., 2007). *p38alpha*-deficient mice are susceptible to carcinogens, and *p38alpha* negatively regulates cell proliferation by antagonizing the *JNK-c-Jun* pathway in multiple cell types and in liver cancer development (Hui et al., 2007a, 2007b). Therefore, upregulation of genes involved in the *p38 Mapk*-network might be a tumor-suppressive action against DNA damage stimulus in the liver following repeated doses of carcinogens. Furthermore, these genes might be useful indicators in the early stage of hepatocarcinogenesis. The *Myc* oncogene is a transcription factor that plays an important role in the pathogenesis of hepatocellular carcinoma (Calvisi and Thorgeirsson, 2005; Thorgeirsson and Grisham, 2002). *Myc* overexpression is believed to exert its neoplastic function via several mechanisms, such as inducing autonomous cell proliferation and growth, blocking differentiation, and causing genomic destabilization (Dang, 1999; Felsher and Bishop, 1999; Grandori et al., 2000; Oster et al., 2002; Pelengaris et al., 2002). While the detailed biological significance should be determined in further studies, several genes were up or downregulated in this network. Among the genes involved in these networks, there is increasing evidence supporting their involvement in carcinogenesis. *Cdh13* (T-cadherin), an atypical member of the cadherin family, is thought to affect cellular biological processes largely via its signaling properties. It is often downregulated in cancerous cells, which is associated with a poor prognosis in various human carcinomas (Andreeva and Kutuzov, 2010). It is also reported that *Cdh13* re-expression in cancer cell lines inhibits cell proliferation and invasiveness, increases susceptibility to apoptosis, and reduces tumor growth (Andreeva and Kutuzov, 2010). Approximately 50% of human hepatocellular carcinomas overexpress *Cdh13* (Riou et al., 2006). While *Cdh13* expression is restricted to endothelial cells from large blood vessels in normal livers, it is upregulated in sinusoidal endothelial cells in invasive hepatocellular carcinomas (Riou et al., 2006). B7-H3 (*Cd276* protein), a surface immunomodulatory glycoprotein, inhibits the functions of natural killer cells and T cells. Whereas the B7-H3 transcript is ubiquitously expressed in various types of human solid tumors as well as normal tissues, the B7-H3 protein is preferentially expressed only in tumor tissues (Xu et al., 2009). While additional biological studies would be required for further confirmation of the biological significance of the modulation of genes involved in these networks, these gene expression changes might play pivotal roles in the early stage of hepatocarcinogenesis.

It is well-known that carcinogenicity is dependent on total exposure levels of compounds; therefore, we have compared total exposure levels of compounds between our experimental conditions and the 2-year bioassay for a better understanding of the toxicological significance of positive results by our prediction model. Due to the abundant literature on carcinogenesis studies, we selected 2 representative hepatocarcinogens, nitrosodiethylamine and acetamidofluorene, for detailed discussions. In our experimental condition, positive predictions for the nitrosodiethylamine and acetamidofluorene groups were observed at cumulative total doses of 240 to 450 mg/kg for nitrosodiethylamine and 420 to 8400 mg/kg for acetamidofluorene. Williams et al. (2004) performed a series of dose-response investigations with these 2 compounds to characterize differences in hepatocarcinogenic effects with respect to exposures. In their two-stage hepatocarcinogenesis study of rats, nitrosodiethylamine was weekly dosed at 40.9 mg/kg for 10 weeks, and a cumulative nitrosodiethylamine dose of 409 mg/kg yielded an 80% hepatocellular tumor incidence followed by 4 weeks of recovery and 24 weeks of promotion with phenobarbital. In contrast, another study demonstrated that a cumulative dose of 409 mg/kg induced a 45% hepatic tumor incidence after 130 weeks of exposure in drinking water (Peto et al., 1991a, 1991b). Regarding acetamidofluorene, a 100% incidence of hepatic tumors was reported at cumulative doses of 282 mg/kg (3.4 mg/kg/day for 12 weeks) followed by 24 weeks of promotion with phenobarbital, while the dose of 1772 mg/kg (3.3 mg/kg/day for 76 weeks) was needed without the promotion (Williams et al., 1991). Although there were some differences in the susceptibility to tumor occurrence in these 2 reports, the cumulative doses of nitrosodiethylamine and acetamidofluorene in our present study were sufficiently above the cumulative dose needed for hepatocarcinogenesis in rats. Taken together, it might be reasonable to conclude that sufficient initiation effects have been achieved under our current dosing conditions of hepatocarcinogens with positive prediction. For building

Table 3
Prediction performance of previously published models.

Models	# of probes	AUC	Sensitivity	False positive rate	Specificity	Correct classification rate
Our current new model	9	0.996	0.990	0.033	0.967	0.978
Our previous model	112	0.983	0.997	0.087	0.913	0.955
Model 1 (Auerbach)	11	0.977	0.960	0.053	0.947	0.953
Model 2 (Ellinger)	101	0.980	0.937	0.057	0.943	0.940
Model 3 (Fielden)	35	0.923	0.830	0.040	0.960	0.895
Model 4(Nakayama)	56	0.982	0.917	0.053	0.947	0.932

models, we have anchored on available carcinogenicity results from 2-year rat bioassays of each compound. Our toxicogenomics project does not only focus on the carcinogenicity of compounds; therefore, SD rats were used as experimental animals in our project, while carcinogenicity tests generally use F344 rats. In addition, rats received orally or intravenously administered compound at the 1-month maximum tolerated doses. However, other dosing methods, generally in the diet or water, are also used for repeated exposure during the 2-year lifespan of rats. Therefore, differences in experimental conditions should be taken into account for a precise comparison. Since we hypothesized that expression changes in our feature genes might reflect the initiated condition of the liver following large doses of carcinogens for up to 1 month, we are conducting further biological studies by using a 2-step carcinogenicity study model in rats. Further data will be published in the near future.

In conclusion, we constructed a new toxicogenomic model for early prediction for both genotoxic and non-genotoxic hepatocarcinogens by using comprehensive gene expression data stored in our large-scale toxicogenomics database. The usefulness and robustness of our predictor were further confirmed in an independent validation data set obtained from a public database. Our toxicogenomic model might be useful for the prospective screening of hepatocarcinogenicity of compounds and prioritization of compounds for carcinogenicity testing. Furthermore, these characteristics of gene expression changes would help to elucidate the mechanisms of action involved in hepatocarcinogenesis.

Conflict of interest statement

The authors have declared no conflict of interest.

Acknowledgment

These studies were supported by a grant from the Ministry of Health, Labour and Welfare of Japan (H14-Toxico-001 and H19-Toxico-001).

Appendix A. Supplementary data

Supplementary data to this article can be found online at doi:10.1016/j.taap.2011.07.001.

References

Andreeva, A.V., Kutuzov, M.A., 2010. Cadherin 13 in cancer. Genes Chromosomes Cancer 49, 775–790.
Auerbach, S.S., Shah, R.R., Mav, D., Smith, C.S., Walker, N.J., Vallant, M.K., Boorman, G.A., Irwin, R.D., 2010. Predicting the hepatocarcinogenic potential of alkenylbenzene flavoring agents using toxicogenomics and machine learning. Toxicol. Appl. Pharmacol. 243, 300–314.
Battershill, J.M., 2005. Toxicogenomics: regulatory perspective on current position. Hum. Exp. Toxicol. 24, 35–40.
Calvisi, D.F., Thorgeirsson, S.S., 2005. Molecular mechanisms of hepatocarcinogenesis in transgenic mouse models of liver cancer. Toxicol. Pathol. 33, 181–184.
Campbell, J.S., Argast, G.M., Yuen, S.Y., Hayes, B., Fausto, N., 2011. Inactivation of p38 MAPK during liver regeneration. Int. J. Biochem. Cell Biol. 43, 180–188.
Chen, J.J., Tsai, C., Tzeng, S., Chen, C., 2007. Gene selection with multiple ordering criteria. BMC Bioinformatics 8, 74.
Dang, C.V., 1999. c-Myc target genes involved in cell growth, apoptosis, and metabolism. Mol. Cell. Biol. 19, 1–11.
Ellinger-Ziegelbauer, H., Gmuender, H., Bandenburg, A., Ahr, H.J., 2008. Prediction of a carcinogenic potential of rat hepatocarcinogens using toxicogenomics analysis of short-term in vivo studies. Mutat. Res. 637, 23–39.
Felsher, D.W., Bishop, J.M., 1999. Transient excess of MYC activity can elicit genomic instability and tumorigenesis. Proc. Natl. Acad. Sci. U.S.A. 96, 3940–3944.
Fielden, M.R., Brennan, R., Gollub, J., 2007. A gene expression biomarker provides early prediction and mechanistic assessment of hepatic tumor induction by nongenotoxic chemicals. Toxicol. Sci. 99, 90–100.
Fielden, M.R., Nie, A., McMillian, M., Elangbam, C.S., Trela, B.A., Yang, Y., Dunn II, R.T., Dragan, Y., Fransson-Stehen, R., Bogdanffy, M., Adams, S.P., Foster, W.R., Chen, S.J., Rossi, P., Kasper, P., Jacobson-Kram, D., Tatsuoka, K.S., Wier, P.J., Gollub, J., Halbert, D.N., Roter, A., Young, J.K., Sina, J.F., Marlowe, J., Martus, H.J., Aubrecht, J., Olaharski, A.J., Roome, N., Nioi, P., Pardo, I., Snyder, R., Perry, R., Lord, P., Mattes, W., Car, B.D., Predictive Safety Testing Consortium, Carcinogenicity Working Group, 2008. Interlaboratory evaluation of genomic signatures for predicting carcinogenicity in the rat. Toxicol. Sci. 103, 28–34.
Gao, W., Mizukawa, Y., Nakatsu, N., Minowa, Y., Yamada, H., Ohno, Y., Urushidani, T., 2010. Mechanism-based biomarker gene sets for glutathione depletion-related hepatotoxicity in rats. Toxicol. Appl. Pharmacol. 247, 211–221.
Grandori, C., Cowley, S.M., James, L.P., Eisenman, R.N., 2000. The Myc/Max/Mad network and the transcriptional control of cell behavior. Annu. Rev. Cell. Dev. Biol. 16, 653–699.
Heinloth, A.N., Irwin, R.D., Boorman, G.A., Nettesheim, P., Fannin, R.D., Sieber, S.O., Snell, M.L., Tucker, C.J., Li, L., Travlos, G.S., Vansant, G., Blackshear, P.E., Tennant, R.W., Cunningham, M.L., Paules, R.S., 2004. Gene expression profiling of rat livers reveals indicators of potential adverse effects. Toxicol. Sci. 80, 193–202.
Hirode, M., Ono, A., Miyagishima, T., Nagao, T., Ohno, Y., Urushidani, T., 2008. Gene expression profiling in rat liver treated with compounds inducing phospholipidosis. Toxicol. Appl. Pharmacol. 229, 290–299.
Hui, L., Bakiri, L., Stepniak, E., Wagner, E.F., 2007a. p38alpha: a suppressor of cell proliferation and tumorigenesis. Cell Cycle 6, 2429–2433.
Hui, L., Bakiri, L., Mairhorfer, A., Schweifer, N., Haslinger, C., Kenner, L., Komnenovic, V., Scheuch, H., Beug, H., Wagner, E.F., 2007b. p38alpha suppresses normal and cancer cell proliferation by antagonizing the JNK-c-Jun pathway. Nat. Genet. 39, 741–749.
Irwin, R.D., Boorman, G.A., Cunningham, M.L., Heinloth, A.N., Malarkey, D.E., Paules, R.S., 2004. Application of toxicogenomics to toxicology: basic concepts in the analysis of microarray data. Toxicol. Pathol. 32, 72–83.
Karin, M., Lawrence, T., Nizet, V., 2006. Innate immunity gone awry: linking microbial infections to chronic inflammation and cancer. Cell 124, 823–835.
Kiyosawa, N., Ando, Y., Manabe, S., Yamoto, T., 2009. Toxicogenomic biomarkers for liver toxicity. J. Toxicol. Pathol. 22, 35–52.
Kondo, C., Minowa, Y., Uehara, T., Okuno, Y., Nakatsu, N., Ono, A., Maruyama, T., Kato, I., Yamate, J., Yamada, H., Ohno, Y., Urushidani, T., 2009. Identification of genomic biomarkers for concurrent diagnosis of drug-induced renal tubular injury using a large-scale toxicogenomics database. Toxicology 265, 15–26.
Kramer, J.A., Curtiss, S.W., Kolaja, K.L., Alden, C.L., Blomme, E.A., Curtiss, W.C., Davila, J.C., Jackson, C.J., Bunch, R.T., 2004. Acute molecular markers of rodent hepatic carcinogenesis identified by transcription profiling. Chem. Res. Toxicol. 17, 463–470.
Kumar, S., Boehm, J., Lee, J.C., 2003. p38 MAP kinases: key signalling molecules as therapeutic targets for inflammatory diseases. Nat. Rev. Drug Discov. 2, 717–726.
Matsumoto, H., Yakabe, Y., Saito, K., Sumida, K., Sekijima, M., Nakayama, K., Miyaura, H., Saito, F., Otsuka, M., Shirai, T., 2009. Discrimination of carcinogens by hepatic transcript profiling in rats following 28-day administration. Cancer Inform. 7, 253–269.
Nakayama, K., Kawano, Y., Kawakami, Y., Moriwaki, N., Sekijima, M., Otsuka, M., Yakabe, Y., Miyaura, H., Saito, K., Sumida, K., Shirai, T., 2006. Differences in gene expression profiles in the liver between carcinogenic and non-carcinogenic isomers of compounds given to rats in a 28-day repeat-dose toxicity study. Toxicol. Appl. Pharmacol. 217, 299–307.
Naugler, W.E., Sakurai, T., Kim, S., Maeda, S., Kim, K., Elsharkawy, A.M., Karin, M., 2007. Gender disparity in liver cancer due to sex differences in MyD88-dependent IL-6 production. Science 317, 121–124.
Nie, A.Y., McMillian, M., Parker, J.B., Leone, A., Bryant, S., Yieh, L., Bittner, A., Nelson, J., Carmen, A., Wan, J., Lord, P.G., 2006. Predictive toxicogenomics approaches reveal underlying molecular mechanisms of nongenotoxic carcinogenicity. Mol. Carcinog. 45, 914–933.
Oster, S.K., Ho, C.S., Soucie, E.L., Penn, L.Z., 2002. The myc oncogene: MarvelouslY Complex. Adv. Cancer Res. 84, 81–154.
Pelengaris, S., Khan, M., Evan, G., 2002. c-MYC: more than just a matter of life and death. Nat. Rev. Cancer 2, 764–776.
Peto, R., Gray, R., Brantom, P., Grasso, P., 1991a. Effects on 4080 rats of chronic ingestion of N-nitrosodiethylamine or N-nitrosodimethylamine: a detailed dose-response study. Cancer Res. 51, 6415–6451.
Peto, R., Gray, R., Brantom, P., Grasso, P., 1991b. Dose and time relationships for tumor induction in the liver and esophagus of 4080 inbred rats by chronic ingestion of N-nitrosodiethylamine or N-nitrosodimethylamine. Cancer Res. 51, 6452–6469.
Riou, P., Saffroy, R., Chenailler, C., Franc, B., Gentile, C., Rubinstein, E., Resink, T., Debuire, B., Piatier-Tonneau, D., Lemoine, A., 2006. Expression of T-cadherin in tumor cells influences invasive potential of human hepatocellular carcinoma. FASEB J. 20, 2291–2301.
Searfoss, G.H., Ryan, T.P., Jolly, R.A., 2005. The role of transcriptome analysis in pre-clinical toxicology. Curr. Mol. Med. 5, 53–64.
Thorgeirsson, S.S., Grisham, J.W., 2002. Molecular pathogenesis of human hepatocellular carcinoma. Nat. Genet. 31, 339–346.
Uehara, T., Hirode, M., Ono, A., Kiyosawa, N., Omura, K., Shimizu, T., Mizukawa, Y., Miyagishima, T., Nagao, T., Urushidani, T., 2008. A toxicogenomics approach for early assessment of potential non-genotoxic hepatocarcinogenicity of chemicals in rats. Toxicology 250, 15–26.
Uehara, T., Ono, A., Maruyama, T., Kato, I., Yamada, H., Ohno, Y., Urushidani, T., 2010. The Japanese toxicogenomics project: application of toxicogenomics. Mol. Nutr. Food Res. 54, 218–227.
Urushidani, T., 2010. Toxicogenomics project and drug safety evaluation. Nippon Yakurigaku Zasshi 136, 46–49.
Williams, G.M., Tanaka, T., Maruyama, H., Maeura, Y., Weisburger, J.H., Zang, E., 1991. Modulation by butylated hydroxytoluene of liver and bladder carcinogenesis induced by chronic low level exposure to 2-acetylaminofluorene. Cancer Res. 51, 6224–6230.
Williams, G.M., Iatropoulous, M.J., Jeffrey, A.M., 2004. Thresholds for the effects of 2-acetylaminofluorene in rat liver. Toxicol. Pathol. 32, 85–91.
Xu, H., Cheung, I.Y., Guo, H.F., Cheung, N.K., 2009. MicroRNA miR-29 modulates expression of immunoinhibitory molecule B7-H3: potential implications for immune based therapy of human solid tumors. Cancer Res. 69, 6275–6281.

Toxicology 295 (2012) 1–7

Contents lists available at SciVerse ScienceDirect

Toxicology

journal homepage: www.elsevier.com/locate/toxicol

Identification of a novel set of biomarkers for evaluating phospholipidosis-inducing potential of compounds using rat liver microarray data measured 24-h after single dose administration

Henrik T. Yudate[a,1], Toshihiro Kai[a,*,1], Mikio Aoki[a], Yohsuke Minowa[b], Toru Yamada[a], Toru Kimura[a], Atsushi Ono[c], Hiroshi Yamada[b], Yasuo Ohno[d], Tetsuro Urushidani[b,e]

[a] Genomic Science Laboratories, Dainippon Sumitomo Pharma Co., Ltd., Japan
[b] Toxicogenomics Informatics Project, National Institute of Biomedical Innovation, Japan
[c] Division of Risk Assessment, National Institute of Health Sciences, Japan
[d] National Institute of Health Sciences, Japan
[e] Department of Pathophysiology, Faculty of Pharmaceutical Sciences, Doshisha Women's College of Liberal Arts, Japan

ARTICLE INFO

Article history:
Received 9 February 2012
Accepted 29 February 2012
Available online 7 March 2012

Keywords:
Biomarker
Phospholipidosis
Microarray
Gene expression
Toxicogenomics
Liver

ABSTRACT

Phospholipid accumulation manifests as an adverse effect of cationic amphiphilic drugs in particular. Detection, however, by histopathology examination is time-consuming and may require repeated administration of compounds for several weeks. To eliminate compounds with potential for inducing phospholipidosis from the discovery pipeline, we have identified and validated a set of biomarkers for predicting the phospholipidosis-inducing potential utilizing a comprehensive rat transcriptome microarray database created by the Japanese Toxicogenomics and Toxicogenomics Informatics Projects (TGP/TGP2) together with in-house data. The set of biomarkers comprising 25 Affymetrix GeneChip probe sets was identified using genetic algorithm optimization on 24-h time-point microarray data from rats treated with single doses of hepatotoxic compounds including amiodarone, clomipramine, haloperidol, hydroxyzine, imipramine, and perhexiline. The set of novel biomarkers represents an early time-point gene-expression pattern characteristic for a condition eventually leading to phospholipidosis. This implies significant advantages in terms of time and resources over currently published biomarkers derived using repeated-dosing late time-point data. The biomarker set was validated by 11 independent compounds. Accuracy, sensitivity, and specificity values were 82%, 67%, and 100%, respectively and the area under the receiver operating characteristic curve was 0.97. These results show that the biomarker set possesses a high classification accuracy for novel compounds. Pathway analysis was carried out for the biomarkers and the detection of pathways related to lipid-metabolism was statistically significant. These pathways most probably reflect lipid metabolism changes associated with phospholipidosis supporting the validity of our novel biomarkers.

1. Introduction

Phospholipidosis is an excessive accumulation of phospholipids in lysosomes and may occur in multiple organs and tissues of the body (Anderson and Borlak, 2006; Halliwell, 1997; Hruban, 1984; Reasor and Kacew, 2001). It is characterized by vacuolated cells as seen on light microscopy and by multicentric lamellated membranous inclusions (lamellar bodies) as seen in the cytoplasm on electron microscopy (Anderson and Borlak, 2006; Hruban, 1984). Many cationic amphiphilic drugs (CADs) (including antidepressants, antimicrobial agents, and antiarrhythmic agents) have been reported to induce phospholipidosis, and drug-induced phospholipidosis is a concern of the pharmaceutical industry and regulatory agencies (Berridge et al., 2007; Kruhlak et al., 2008). In the case that phospholipidosis is detected in preclinical studies, a wide margin between drug efficacy and drug toxicity will be required to move forward to clinical development. It is therefore essential to evaluate phospholipidosis-inducing potential of compounds at an early stage in order to reduce the risk of attrition in drug development. Phospholipidosis-inducing potential of compounds is

* Corresponding author. Tel.: +81 6 6466 5201.
E-mail address: tkai@m.u-tokyo.ac.jp (T. Kai).
[1] These authors contributed equally to this work.

0300-483X/$ – see front matter © 2012 Elsevier Ireland Ltd. All rights reserved.
doi:10.1016/j.tox.2012.02.015

generally assessed in pharmaceutical companies by histopathological examination in repeated dose toxicity studies, and consequently alternative methods are required for the early prediction of phospholipidosis.

Analysis of genome-wide gene expression data has been shown in numerous studies to contribute to the elucidation of mechanism of actions of novel compounds, adverse effects (Chiang and Butte, 2009), or induced injuries (Blomme et al., 2009). Pharmaceutical research and development divisions are constantly under pressure to discover and develop new compounds, and we have experienced an increase in both time and cost of this process from the early concept to marketing of a successful drug (DiMasi et al., 2003). It is not surprising, therefore, that companies have embraced gene expression analysis in their portfolio of techniques, and several major Japanese pharmaceutical companies and national institutes have jointly created a database of rat in vivo/in vitro and human in vitro transcriptome microarray data in the Japanese Toxicogenomics and Toxicogenomics Informatics Projects (TGP/TGP2) (Urushidani and Nagao, 2005). Whereas microarray data are also publicly available most notably from the GEO and Stanford microarray databases, the current database from the TGP project represents a unique opportunity for the pharmaceutical industry to analyze compound-induced toxicities with its more than 27,000 Affymetrix chip samples covering several dose and time points for approximately 150 compounds, most of which are drugs that have been shown to induce one or more toxicities.

Structure–activity relationship (SAR) models, phospholipid staining, and biomarker-based approaches have been developed to support evaluation of the phospholipidosis-inducing potential of compounds. SAR models are mainly based on pKa (ionization constant) and cLog P (hydrophobicity) (Kuroda and Saito, 2010; Ploemen et al., 2004), but some processes are difficult to explain by simple parameters (e.g. binding of compounds to phospholipids, inhibition of phospholipid degradation) (Halliwell, 1997; Kuroda and Saito, 2010; Taillardat-Bertschinger et al., 2002). The phospholipid staining approach is suitable for high-throughput screening (HTS) using cultured cell lines, but evaluation of drug metabolite toxicities is difficult with this method (Fujimura et al., 2007; Nioi et al., 2007). Furthermore, the same concentration for all compounds is used in this approach although the organ distribution is different. Finally, several biomarker candidates for evaluation of phospholipidosis-inducing potential of compounds have been reported in previous studies. In particular, di-docosahexaenoyl (C22:6)-bis(monoacylglycerol) phosphate (Baronas et al., 2007; Tengstrand et al., 2010) and phenylacetylglycine (Delaney et al., 2004) may have utility as noninvasive urinary phospholipidosis biomarkers. In a recent toxicogenomic approach, 78 probe-sets of rat hepatic genes were extracted from microarray data measured after repeated dosing. The predictive performance, however, of these biomarkers leave room for improvement, and accurate biomarkers, which can be detected in single-dose toxicity studies, are still highly required (Hirode et al., 2008; Reasor et al., 2006; Sawada et al., 2005).

In the present study, we extracted a set of biomarker candidates to predict phospholipidosis-inducing potential using the comprehensive TGP database. The set of biomarkers was optimized on hepatic gene expression data measured 24 h after single dose administration of individual compounds from this database and subsequently assessed by an external validation set that was not available at the time of biomarker optimization.

2. Materials and methods

2.1. Compounds

The chemical name, abbreviation, dosage, vehicle, administration route, and phospholipidosis-inducing potential are summarized in Table 1 for all compounds used in the present study.

2.2. Animal treatment

Animal treatment has been described previously (Takashima et al., 2006). Five-week-old male Sprague-Dawley rats were purchased from Charles River Japan Inc. (Kanagawa, Japan). After a 7-day quarantine and acclimatization period, 6-week-old animals were assigned to dosage groups using a computerized stratified random grouping method based on individual body weight. The animals were individually housed in stainless-steel cages in a room that was lighted for 12 h (7:00–19:00) daily, ventilated with an air-exchange rate of 15 times per hour, and maintained at 21–25 °C with a relative humidity of 40–70%. Each animal was allowed free access to water and pellet food (CRF-1, sterilized by radiation, Oriental Yeast Co., Japan). Rats in each group were orally administered with various drugs suspended or dissolved either in 0.5% methylcellulose solution (MC) or corn oil according to their dispersibility, except that cephalothin was dissolved in saline and administered intravenously. Animals were sacrificed 24 h after the last dose. The experimental protocols were reviewed and approved by the Ethics Review Committee for Animal Experimentation of the National Institute of Health Sciences.

2.3. Microarray analysis

An aliquot of the tissue sample (approximately 30 mg) for microarray analysis was obtained from the left lateral lobe of the liver in each animal immediately after sacrifice, kept in RNAlater (Ambion, Austin, TX, USA) overnight at 4 °C, and then frozen at −80 °C until use. Liver samples were homogenized with the buffer RLT supplied in RNeasy Mini Kit (Qiagen, Valencia, CA, USA), and total RNA was isolated according to the manufacture's instructions. Microarray experiments were performed using GeneChip® RAT Genome 230 2.0 Arrays (Affymetrix, Santa Clara, CA, USA), containing 31,042 probe-sets. The procedure was conducted according to the manufacturer's instructions for cDNA synthesis, purification, and biotin-labeled cRNA synthesis. Ten micrograms of fragmented cRNA was hybridized to a Rat Genome 230 2.0 Array for 18 h at 45 °C at 60 rpm, after which the array was washed and stained by streptavidin–phycoerythrin using Fluidics Station 400 (Affymetrix) and then scanned with a Gene Array Scanner (Affymetrix). The digital image files were processed with an Affymetrix Microarray Suite version 5.0 (MAS5.0) and the intensities were normalized for each chip by setting the mean intensity to 100. Signal intensities were averaged over three replicates for each dosage groups. Microarray data and histopathological findings from TGP/TGP2 as used in this study have been made publicly available in the Open TG-Gates website (http://toxico.nibio.go.jp/).

2.4. Genetic algorithm

Our group hypothesized that compounds with the capability to induce phospholipidosis possibly give rise to a characteristic gene expression pattern leading to phospholipid accumulation and that this pattern may exist at a time point much earlier than the time point at which phospholipidosis can be confirmed in histopathology analysis. We therefore set out to identify a distinguishing pattern by developing a genetic algorithm (Golub et al., 1999) and applied it to single-dose 24-h gene expression data. The gene expression data were initially filtered both for fold change relative to vehicle and for expression level. We used a signal expression threshold of 300.0 and a fold change criteria of 1.6. The genetic algorithm was set up with a population of 50 chromosomes each representing a set of 25 marker candidates, which were initially selected at random. The mutation rate and crossover probability were set to 0.1 and 0.8, respectively, which may be commonly used values. Average fold change values of marker candidates were computed as follows. For each marker candidate, the number of positive training set compounds in which the marker was increased (a), decreased (b), and not changed (c) were counted. If (a) was greater than (b), the fold change value was computed as the average over positive compounds in which the marker was increased. If (b) was greater than (a), the fold change value was computed as the average over positive compounds in which the marker was decreased. If (a) was equal to (b), the marker would not be a candidate for optimization. The phospholipidosis signature was defined as the set of the logarithm of the average fold change values computed as described above for the marker candidates. The fitness function in the genetic algorithm computes the Pearson correlation coefficient between the phospholipidosis signature and the logarithm of fold change values obtained from the training set samples for the set of selected marker candidates (see Table 3). A total of 25,000 generations were generated at which point the fitness values did no longer change. Accordingly, 1,250,000 chromosomes, i.e., sets of marker candidates, were evaluated in a single optimization cycle. The genetic algorithm optimized the fitness function as described above, it was required that all training set compounds should be correctly evaluated, and that the variance of the fitness values over the positive compounds should be minimized. The phospholipidosis signature was subsequently validated for predicting the phospholipidosis-inducing potential on novel in-house data that were prepared only after the final signature had been selected. This signature and the validation are detailed in the following.

2.5. Assessment with external validation set

Following optimization of the biomarker set for phospholipidosis prediction, an external validation set comprising 11 compounds (Table 1) was used to assess

Table 1
Training set and independent validation set compounds.

Compound	Abbreviation	Dose (mg/kg)	Vehicle	Route	Phospholipidosis induction
Training set					
Azathioprine	AZP	30	MC	p.o.	Negative
Benziodarone	BZD	300	MC	p.o.	Negative
Cephalothin	CLT	2000	Saline	i.v.	Negative
Cimetidine	CIM	1000	MC	p.o.	Negative
Clofibrate	CFB	300	Corn oil	p.o.	Negative
Colchicine	COL	15	MC	p.o.	Negative
Cyclosporine A	CSA	300	Corn oil	p.o.	Negative
Danazol	DNZ	2000	MC	p.o.	Negative
Diltiazem	DIL	800	MC	p.o.	Negative
Disopyramide	DIS	400	MC	p.o.	Negative
Enalapril	ENA	600	MC	p.o.	Negative
Famotidine	FAM	1000	MC	p.o.	Negative
Glibenclamide	GBC	1000	Corn oil	p.o.	Negative
Ibuprofen	IBU	400	MC	p.o.	Negative
Mefenamic acid	MEF	300	MC	p.o.	Negative
Metformin	MEM	1000	MC	p.o.	Negative
Omeprazole	OPZ	1000	MC	p.o.	Negative
Phenytoin	PHE	600	MC	p.o.	Negative
Quinidine	QND	200	MC	p.o.	Negative
Rifampicin	RIF	200	MC	p.o.	Negative
Tacrine	TAC	30	MC	p.o.	Negative
Amiodarone	AM	200	MC	p.o.	Positive
Clomipramine	CPM	100	MC	p.o.	Positive
Haloperidol	HPL	30	MC	p.o.	Positive
Hydroxyzine	HYZ	100	MC	p.o.	Positive
Imipramine	IMI	100	MC	p.o.	Positive
Perhexiline	PH	150	MC	p.o.	Positive
Independent validation set					
Cyproterone	CP	100	Corn oil	p.o.	Negative
Diflunisal	DF	100	MC	p.o.	Negative
Doxycycline	DOX	250	MC	p.o.	Negative
Ofloxacin	OFL	200	MC	p.o.	Negative
Procainamide	PROC	50	MC	p.o.	Negative
Chloroquine	CQ	100	MC	p.o.	Positive
Citalopram	CTP	150	Corn oil	p.o.	Positive
Clozapine	CLZ	100	MC	p.o.	Positive
Fluoxetine	FLX	100	MC	p.o.	Positive
Maprotiline	MPT	150	MC	p.o.	Positive
Zimelidine	ZIM	100	MC	p.o.	Positive

MC, 0.5 w/v% methylcellulose; p.o., peroral; i.v., intravenous.

the accuracy, sensitivity, and specificity of the final model. The external validation data were obtained from experiments conducted in-house, and they are therefore independent of the TGP database. We purchased rats that were identical in terms of strain, age, and supplier, and employed the same Affymetrix GeneChip system, whereas the laboratory in which the actual experiments were performed, the lots of reagents, and the technicians in charge differed.

In order to calculate the receiver operating characteristic (ROC) curves, we used the ROC function of the Epi package (Carstensen, 2007) included in the statistical software R (version 2.13.0.).

2.6. Pathway analysis

The Ingenuity Pathways Analysis software (IPA® 8.5, Ingenuity Systems, www.ingenuity.com) was used to identify any presence of significant canonical pathways in the final set of biomarkers.

3. Results

3.1. Sample selection and liver histopathology

Six compounds known to induce phospholipidosis (AM, CPM, HPL, HYZ, IMI, and PH) were selected as the positive part of the training set (Table 1). Vacuolization was observed in the livers after repeated administration of AM (for 7–28 days), CPM (for 28 days), HYZ (for 14–28 days), and IMI (for 7–28 days). In the case of HPL and PH, no vacuolization was seen after repeated administration for 28 days under our assay conditions. These compounds, however, have been confirmed to induce phospholipidosis as reported in the literature (Table 2) (Atienzar et al., 2007; Kasahara et al., 2006; Pelletier et al., 2007; Tomizawa et al., 2006). Twenty-one compounds, which have not been reported to be related to phospholipidosis, were chosen for the negative part of the training set. The compounds were selected from among the remaining TGP compounds, considering diversity in both molecular structure and toxicity (Table 1).

3.2. Biomarker discovery

In order to develop a biomarker model for prediction of phospholipidosis-inducing potential using hepatic gene expression data measured only 24 h after single dose administration, we applied the genetic algorithm to the training set of 21 negative and 6 positive compounds (Table 1), as described in Section 2. The optimization resulted in a set of biomarkers, i.e., a phospholipidosis signature. The phospholipidosis signature itself is listed in Table 3 as annotated with Affymetrix probe set identifiers, gene symbols and gene titles. A phospholipidosis score for an individual compound is computed as Pearson's correlation coefficient between the phospholipidosis signature and the logarithm of the fold change values obtained from the compound. The calculated values for all positive compounds in the training set are listed in Table 3. The phospholipidosis signature was capable of correctly characterizing each of the training set compounds regarding phospholipidosis-inducing potential (Fig. 1). It was necessary to introduce a threshold for the phospholipidosis score using the training set data in order to be able

Table 2
Histopathological findings and references for 6 positive training set compounds.

Compound	Findings	Topography	24 h	4 day	8 day	15 day	29 day	Reference
Amiodarone	Vacuolization	Bile duct cell	(−)	(−)	3/5 (±)	1/5 (±), 4/5 (+)	4/4 (+)	1, 2, 3, 4
	Vacuolization	Hepatocyte	(−)	(−)	(−)	2/5 (±)	4/4 (±)	
	Vacuolization	Kupper cell	(−)	(−)	(−)	5/5 (±)	4/4 (±)	
Clomipramine	Vacuolization	Hepatocyte	(−)	(−)	(−)	(−)	1/5 (±), 1/5 (+)	1, 2, 3, 4
Haloperidol	Not applicable	Not applicable	(−)	(−)	(−)	(−)	(−)	3, 4
Hydroxyzine	Vacuolization	Hepatocyte	(−)	(−)	(−)	2/5 (±), 2/5 (+)	4/5 (+), 1/5 (2+)	1
Imipramine	Vacuolization	Hepatocyte	(−)	(−)	4/5 (±)	1/5 (±), 2/5 (+)	1/4 (±), 3/4 (+)	1, 2, 3
	Vacuolization	Kupper cell	(−)	(−)	(−)	3/5 (±)	(−)	
Perhexiline	Not applicable	Not applicable	(−)	(−)	(−)	(−)	(−)	1, 2, 4

−, negative; ±, minimal; +, slight; 2+, moderate; 3+, severe.
References: (1) Pelletier et al. (2007); (2) Tomizawa et al. (2006); (3) Kasahara et al. (2006); (4) Atienzar et al. (2007).

to make objective decisions when the phospholipidosis signature is applied to novel data. As seen in Fig. 1, any threshold value in the range from 0.48 to 0.60 separates the scores from the positive and negative compounds and the intermediate value 0.54 is therefore adequate as an objective threshold.

The result of the IPA canonical pathway analysis on the set of 25 biomarkers is listed in Table 4. The most significantly represented pathway is the Metabolism of Xenobiotics by Cytochrome P450, as is also evident from the list of individual biomarkers in Table 3, where several P450 and UGT enzymes are present. The following three pathways "linoleic acid metabolism", "fatty acid metabolism", and "arachidonic acid metabolism" from the IPA analysis are indeed related to lipid metabolism underscoring the hypothesis that there exist characteristic genes exhibiting an early gene expression pattern leading to phospholipidosis. These pathways most probably reflect the change of lipid metabolism in association with phospholipidosis.

3.3. *Validation using the external data set*

The predictive performance of the novel set of biomarkers derived in the present study was assessed by data from an

Table 3
List of 25 probe sets for evaluation of phospholipidosis-inducing potential at 24 h following single dose oral administration.

Probe set ID	Gene symbol	Gene title	Phospholipidosis signature (a)	Log 2 of fold-change values (b)					
				AM	CPM	HPL	HYZ	IMI	PH
1367691_at	Prkcdbp	UDP glucuronosyltransferase 2 family, polypeptide B17	−0.872	0.441	0.254	−1.037	0.202	0.381	−0.724
1368155_at	Cyp2c12	Cytochrome P450, family 2, subfamily c, polypeptide 12	−1.315	0.162	−0.925	−1.977	0.142	−0.334	−1.234
1368453_at	Fads2	Fatty acid desaturase 2	−1.088	−0.207	−0.474	−1.442	−0.524	−0.363	−0.803
1370281_at	Fabp5	Fatty acid binding protein 5, epidermal	−1.172	−1.087	−0.613	−1.950	−0.850	−1.240	−0.881
1370350_x_at	Rup2	Urinary protein 2	−0.754	0.361	−0.665	0.303	−0.761	−0.748	−0.039
1370387_at	Cyp3a9	Cytochrome P450, family 3, subfamily a, polypeptide 9	1.301	0.447	1.619	0.816	1.592	0.520	0.662
1370698_at	Ugt2b17	UDP glucuronosyltransferase 2 family, polypeptide B17	1.510	0.321	1.494	0.439	1.480	1.555	0.041
1371076_at	Cyp2b1/2b2	Cytochrome P450, family 2, subfamily b, polypeptide 1/2	2.094	0.399	1.644	1.019	3.244	2.272	0.402
1371390_at	Tubb2c	Tubulin, beta 2c	−0.838	−0.886	−0.136	−0.925	0.261	−0.756	−0.063
1371479_at	Mettl7a	Methyltransferase like 7A	0.810	0.451	0.000	0.914	0.609	0.698	0.514
1371942_at	Gstt3	Glutathione S-transferase theta 3	1.278	0.605	−0.351	1.671	0.673	1.492	0.720
1372585_at	RGD1566254	RGD1566254	0.838	0.749	0.765	−0.740	−0.180	−0.188	−0.132
1372727_at	–	EST	−1.003	−0.089	−1.229	−0.809	−0.359	−0.575	0.630
1373992_at	MGC108823	Similar to interferon-inducible GTPase	1.044	0.863	0.710	−0.361	0.079	−0.654	−0.183
1377950_at	RGD1309362	Similar to interferon-inducible GTPase	−1.606	0.354	−0.644	−3.322	−1.613	0.503	−0.840
1378260_at	Adh1	Alcohol dehydrogenase 1	−0.814	−0.166	0.468	0.621	−0.855	−0.061	−0.773
1379888_at	–	EST	0.990	0.113	−0.771	1.239	−0.242	0.889	0.804
1384580_at	C6	Complement component 6	−0.912	−0.158	0.150	−1.187	−0.298	−0.681	0.340
1387093_at	Slco1a4	Solute carrier organic anion transporter family, member 1a4	−0.912	0.695	0.441	0.010	1.247	0.795	0.815
1387094_at	Slco1a4	Solute carrier organic anion transporter family, member 1a4	1.030	0.713	0.656	−0.030	1.322	1.064	0.928
1387865_at	Dut	Deoxyuridine triphosphatase	−0.844	−0.601	−0.306	−1.014	0.185	−0.692	−0.410
1387892_at	Tubb5	Tubulin, beta 5	−0.940	−0.957	−0.240	-1.092	0.227	−1.055	−0.436
1388318_at	Pgk1	Phosphoglycerate kinase 1	0.848	−0.389	−0.039	0.038	0.764	0.928	−0.077
1389967_at	Arl6ip1	AD-ribosylation factor-like 6 interacting protein 1	−0.753	−0.385	−0.273	−0.741	0.341	−0.764	−0.062
1398307_at	Cyp3a18	Cytochrome P450, 3a18	1.057	0.485	−0.245	0.353	1.179	0.016	0.924
Phospholipidosis scores[a]				0.60	0.67	0.78	0.77	0.74	0.70

[a] Phospholipidosis scores are computed as Pearson's correlation coefficients between (a) and (b).